polymyositis/dermatomyositis (PM/DM) patients (n = 10) were negative. In addition, in the synovial fluid of a subset of RA patients, we detected $CD4^+$ T cells producing IFN-γ upon stimulation with RPL23A (Fig. 4, D and E). These findings in humans, together with the key role of anti-RPL23A T cell responses for autoimmune arthritis and psoriasis-like dermatitis in mice, suggest that the responses may play a pathogenic role at least in a subset of patients with RA or PsA.

Our results show that by attenuating TCR signal intensity in developing T cells (hence reducing their sensitivity to thymic negative selection by natural self ligands), T cells reactive with ubiquitously expressed self antigens can be generated as dominant pathogenic clones causing systemic autoimmune disease. Because similar attenuation of TCR signaling at various degrees in conjunction with T_{reg} cell depletion is able to produce a variety of other autoimmune diseases in mice (*9*, *22*), this strategy of generating pathogenic T cells and characterizing the self antigens they recognize would facilitate our understanding of the mechanisms of other autoimmune diseases of currently unknown etiology. In addition, given that genetic polymorphism in a signaling molecule in T cells is a major determinant of genetic susceptibility to various human autoimmune diseases including RA (*23*), such a genetic variation might, at least in part, alter thymic selection, hence forming a TCR repertoire for causing autoimmune disease. Our approach may also be useful in deciphering how T cell autoimmunity to a ubiquitous self antigen triggers localized tissue damage in RA and other human autoimmune diseases, and in devising effective means of systemic or local intervention in the disease process.

REFERENCES AND NOTES

1. S. Sakaguchi, F. Powrie, R. M. Ransohoff, *Nat. Med.* **18**, 54–58 (2012).
2. P. Marrack, J. Kappler, B. L. Kotzin, *Nat. Med.* **7**, 899–905 (2001).
3. M. Feldmann, F. M. Brennan, R. N. Maini, *Cell* **85**, 307–310 (1996).
4. G. S. Firestein, *Nature* **423**, 356–361 (2003).
5. I. B. McInnes, G. Schett, *N. Engl. J. Med.* **365**, 2205–2219 (2011).
6. C. X. Chang *et al.*, *Front. Biosci.* **16**, 3014–3035 (2011).
7. L. Y. Hsu, Y. X. Tan, Z. Xiao, M. Malissen, A. Weiss, *J. Exp. Med.* **206**, 2527–2541 (2009).
8. N. Sakaguchi *et al.*, *Nature* **426**, 454–460 (2003).
9. S. Tanaka *et al.*, *J. Immunol.* **185**, 2295–2305 (2010).
10. C. L. Sommers *et al.*, *Science* **296**, 2040–2043 (2002).
11. O. M. Siggs *et al.*, *Immunity* **27**, 912–926 (2007).
12. J. Holst *et al.*, *Nat. Protoc.* **1**, 406–417 (2006).
13. G. P. Lennon *et al.*, *Immunity* **31**, 643–653 (2009).
14. M. L. Bettini, M. Bettini, M. Nakayama, C. S. Guy, D. A. Vignali, *Nat. Protoc.* **8**, 1837–1840 (2013).
15. See supplementary materials on *Science* Online.
16. F. O. Nestle, D. H. Kaplan, J. Barker, *N. Engl. J. Med.* **361**, 496–509 (2009).
17. K. Suzuki, I. G. Wool, *J. Biol. Chem.* **268**, 2755–2761 (1993).
18. W. Fan, M. Christensen, E. Eichler, X. Zhang, G. Lennon, *Genomics* **46**, 234–239 (1997).
19. W. J. van Venrooij, J. J. van Beers, G. J. Pruijn, *Nat. Rev. Rheumatol.* **7**, 391–398 (2011).
20. K. Hirota *et al.*, *J. Exp. Med.* **204**, 41–47 (2007).
21. M. Hashimoto *et al.*, *J. Exp. Med.* **207**, 1135–1143 (2010).
22. M. Ono, J. Shimizu, Y. Miyachi, S. Sakaguchi, *J. Immunol.* **176**, 4748–4756 (2006).
23. N. Bottini, T. Vang, F. Cucca, T. Mustelin, *Semin. Immunol.* **18**, 207–213 (2006).

ACKNOWLEDGMENTS

We thank D. O. Adeegbe, Y. Kitagawa, and K. Chen for critical reading of the manuscript; E. Yamamoto, M. Matsuura, R. Ishii, Y. Tada, Y. Funabiki, the technical support team (Graduate School of Medicine, Kyoto University), and K. Saito of DNA-chip Development Center for Infectious Diseases (RIMD, Osaka University) for technical assistance; T. Matsushita for histology; T. Kitamura for gifts of the packaging cell line Plat-E; the members of the Department of Rheumatology and Clinical Immunology, Kyoto University, for providing us with patients' sera; and the members of our laboratories for comments. The data presented in this paper are tabulated in the main paper and in the supplementary materials. eFOX mice and plasmids for making retrogenic mice are subject to a material transfer agreement. A patent application related to the work in this paper has been filed (PCT/JP2014/069306: A way to diagnose autoimmune arthritis; Y.I. and S.S. as inventors). Supported by Grants-in-Aid for Specially Promoted Research 20002007 (S.S. and Y.I.),;for Young Scientists (B) 24790996 (Y.I.) from the Japan Society for the Promotion of Science; Core Research for Evolutional Science and Technology from the Japan Science and Technology Agency (S.S.); NIH grant R01 DK089125 (D.A.A.V.); and American Lebanese Syrian Associated Charities (D.A.A.V.). M.H., T.F., M.F., H.I., and T.M. are affiliated with a department that is supported financially by five pharmaceutical companies (Mitsubishi Tanabe Pharma Co., Bristol-Myers K.K., Chugai Pharmaceutical Co. Ltd., AbbVie GK., and Eisai Co. Ltd.). The sponsors were not involved in the study design; in the collection, analysis, or interpretation of data; in the writing of this manuscript; or in the decision to submit the article for publication.

SUPPLEMENTARY MATERIALS

www.sciencemag.org/content/346/6207/363/suppl/DC1
Materials and Methods
Supplementary Text
Figs. S1 to S18
Tables S1 to S3
References (*24*–*36*)

22 July 2014; accepted 16 September 2014
10.1126/science.1259077

Science
AAAS

Detection of T cell responses to a ubiquitous cellular protein in autoimmune disease
Yoshinaga Ito *et al.*
Science **346**, 363 (2014);
DOI: 10.1126/science.1259077

Vaccine 32 (2014) 5901–5907

Contents lists available at ScienceDirect

Vaccine

journal homepage: www.elsevier.com/locate/vaccine

High expression of MAGE-A4 and MHC class I antigens in tumor cells and induction of MAGE-A4 immune responses are prognostic markers of CHP-MAGE-A4 cancer vaccine☆

Takuro Saito[a], Hisashi Wada[a,b,*], Makoto Yamasaki[a], Hiroshi Miyata[a], Hiroyoshi Nishikawa[c], Eiichi Sato[d], Shinichi Kageyama[e], Hiroshi Shiku[e], Masaki Mori[a], Yuichiro Doki[a]

[a] Department of Gastroenterological Surgery, Japan
[b] Department of Clinical Research in Tumor Immunology, Graduate School of Medicine, Japan
[c] Experimental Immunology, Immunology Frontier Research Center Osaka University, Suita, Osaka, Japan
[d] Department of Pathology, Tokyo Medical University, Tokyo, Japan
[e] Departments of Immuno-Gene Therapy and Cancer Vaccine, Mie University, Tsu, Mie, Japan

ARTICLE INFO

Article history:
Received 7 May 2014
Received in revised form 18 July 2014
Accepted 1 September 2014
Available online 13 September 2014

Keywords:
CT antigen
MAGE-A4
Cancer vaccine
Prognosis
MHC
Monitoring

ABSTRACT

Purpose: We conducted a cancer vaccine clinical trial with MAGE-A4 protein. Safety, clinical response, and antigen-specific immune responses were analyzed and the prognostic factors by vaccination were investigated.
Experimental design: Twenty patients with advanced esophageal, stomach or lung cancer were administered MAGE-A4 vaccine containing 300 μg protein subcutaneously once every 2 weeks in six doses. Primary endpoints of this study were safety and MAGE-A4 immune responses.
Results: The vaccine was well tolerated. Fifteen of 20 patients completed one cycle of vaccination and two patients showed SD. A MAGE-A4-specific humoral immune response was observed in four patients who had high expression of MAGE-A4 and MHC class I on tumor cells. These four patients showed significantly longer overall survival than patients without an antibody response after vaccination ($p = 0.009$). Patients with tumor cells expressing high MAGE-A4 or MHC class I antigen showed significantly longer overall survival than those with low expression. Induction of CD4 and CD8T cell responses was observed in three and six patients, respectively, and patients with induction of MAGE-A4-specific IFNγ-producing CD8T cells, but not CD4T cells, lived longer than those without induction.
Conclusions: The CHP-MAGE-A4 vaccine was safe. Expression of MAGE-A4 and MHC class I in tumor tissue and the induction of a MAGE-A4-specific immune response after vaccination would be feasible prognostic markers for patients vaccinated with MAGE-A4.

1. Introduction

The expression of cancer/testis (CT) antigens is normally limited to human germ line cells in the testis and to various types of human cancers [1,2]. Among CT antigens, the melanoma-associated antigen gene (MAGE) family is also known to show such unique expression and to induce spontaneous humoral and cellular immune responses in MAGE-expressing cancer patients [3,4], with the result that they are feasible targets for tumor immunotherapy.

Numerous cancer vaccine strategies are under development and some patients have experienced clinical benefits after vaccination. Among the MAGE family, a phase II cancer vaccine trial with MAGE-A3 protein in non-small-cell lung cancer patients showed 8% reduction of the recurrence rate [5]. Based on the outcome of this phase II study, a randomized double-blind phase III study (MAGRIT trial) with MAGE-A3 protein vaccination was performed [6].

MAGE-A4 is also reported to be expressed in a wide variety of tumors, e.g., 60% esophageal cancer, 50% head and neck cancer, 24% non-small-cell lung cancer, 33% gastric tumor, and 21% Hodgkin's

☆ The study was registered in the University hospital Medical Information Network Clinical Trials Registry (UMIN-CTR) Clinical Trial (Unique trial number: UMIN000003188) on February 15, 2010 (UMIN-CTRURL: http://www.umin.ac.jp/ctr/index.htm).

* Corresponding author at: 2-2 Yamada-oka, Suita, Osaka 565-0871, Japan. Tel.: +81 6 6879 3251; fax: +81 6 6879 3259.
E-mail address: hwada@gesurg.med.osaka-u.ac.jp (H. Wada).

http://dx.doi.org/10.1016/j.vaccine.2014.09.002
0264-410X/

disease but not in normal tissues besides the testis. MAGE-A4 elicits spontaneous humoral or cellular immune responses in patients with MAGE-A4-expressing non-small-cell lung cancer, head and neck cancer and adult T cell leukemia/lymphoma [3,4,7,8]. High expression of MAGE-A4, as well as other CT antigens, in tumors was correlated with the poor prognosis of patients with bladder cancer, ovarian cancer, non-small-cell lung cancer and head and neck cancer [9–14]. Many MAGE-A4 epitope peptides recognized by CD4 and CD8 T cells in the context of human leukocyte antigen (HLA) class I and class II have been identified, e.g., HLA-A0201 [15,16], HLA-A2401 [17], HLA-B3701 [18], HLA-DP0501, and HLA-DR1403 [19].

Because tumor-specific T cells are considered to be a direct effector of tumor immunity, the expression level of MHC class I on cancer cells is crucial for the prognosis of cancer patients, especially in the case of an immune therapy such as a cancer vaccine. It is reported that deficient MHC class I surface expression is associated with reduced patient survival in colon cancer, gastric cancer and non-small-cell lung cancer [20–23], and is considered to be one of the causes of the immune escape of tumor cells [24,25]. In patients vaccinated with tumor antigens, some papers reported the effect of the expression level of MHC class I on cancer cells on the clinical effect of vaccinated patients, but there are few reports on their prognosis after vaccination [26,27].

In this study, we conducted a cancer vaccine clinical trial with a complex of MAGE-A4 protein and cholesteryl pullulan (CHP) nanoparticles in advanced cancer patients. We monitored and analyzed the safety, clinical effect, humoral and cellular immune responses and expression of antigens in these patients.

2. Materials and methods

2.1. CHP-MAGE-A4 vaccine

The complex of cholesterol-bearing hydrophobized pullulan (CHP) and MAGE-A4 protein (CHP-MAGE-A4) was provided by ImmunoFrontier, Inc. (Tokyo, Japan) [28]. The synthesis, production, formulation and packaging of the investigational agent were performed in accordance with current Good Manufacturing Practices (cGMP) and met the applicable criteria for use in humans. The toxicity of the drug products was assessed using animal models, and stability was monitored during the clinical trial using representative samples of the investigational drug product.

2.2. Study design

A phase I, open-label, single-institutional clinical trial of the CHP-MAGE-A4 vaccine was designed to evaluate the safety, immune response and clinical response. Patients eligible for entry were those who had advanced cancers that were refractory to standard therapy and expressed MAGE-A4 antigen as assessed by immunohistochemistry (IHC). The CHP-MAGE-A4 vaccine containing 300 μg MAGE-A4 protein was administered subcutaneously once every 2 weeks in six doses. Two weeks after the last administration, the safety, immune response and clinical response were evaluated. Thereafter, the vaccine was administered additionally. Clinical response was assessed according to the Response Evaluation Criteria in Solid Tumors (RECIST ver1.1) [29]. Safety was evaluated according to the National Cancer Institute Common Terminology Criteria for Adverse Events ver.3.0 (NCI-CTCAE ver.3.0) [30]. The protocol was approved by the Ethics Committee of Osaka Universities according to the Declaration of Helsinki. Written informed consent was obtained from each patient before enrolling in the study. The study was conducted in compliance with Good Clinical Practice and was registered in the University hospital Medical Information Network Clinical Trials Registry (UMIN-CTR) Clinical Trial (Unique trial number: UMIN000003188) on February 15, 2010 (UMIN-CTRURL: http://www.umin.ac.jp/ctr/index.htm).

2.3. MAGE-A4 protein and peptides

For ELISA, recombinant N-His-tagged MAGE-A4 protein was given by Mie University. For Western blot analysis, the MAGE-A4 open reading frame was given by Hokkaido University and was cloned into pGEX-HT plasmid given by Dr. J. Takagi (Osaka University, Osaka, Japan). N-GST-His-tagged MAGE-A4 protein was expressed in M15 *Escherichia coli* cells and purified by Glutathione Sepharose 4B. Finally, recombinant MAGE-A4 protein without a His-tag was purified by TEV protease [31]. For in vitro stimulation of T cells, the following series of 31 MAGE-A4 overlapping peptides spanning the protein was synthesized: 1–20, 11–30, 21–40, 31–50, 41–60, 51–70, 61–80, 71–90, 81–100, 91–110, 101–120, 111–130, 121–140, 131–150, 141–160, 151–170, 161–180, 171–190, 181–200, 191–210, 201–220, 211–230, 221–240, 231–250, 241–260, 251–270, 261–280, 271–290, 281–300, 291–310, and 300–317.

2.4. ELISA

Recombinant protein (0.4 μg/ml) in coating buffer was adsorbed onto 96-well plates and incubated overnight at 4 °C. Plates were washed with phosphate-buffered saline (PBS) and blocked with 1% bovine serum albumin (BSA). 100 μl of serially diluted serum was added to each well and incubated for 2 h at room temperature. Horseradish peroxidase (HRP)-conjugated goat anti-human IgG (Medical & Biological Laboratories, Nagoya, Japan) was added to the wells. Ovalbumin (OVA, albumin from chicken egg white; Sigma, St. Louis, MO) was used as the control protein in each assay. The cut-off value of the antibody reaction was 0.47 O.D., calculated from the results of 47 healthy donors with the average + 2 SD.

2.5. Immunohistochemistry (IHC)

IHC was performed using formalin-fixed paraffin-embedded cancer specimens obtained from all patients enrolled in this trial and 57 esophageal cancer patients who had received surgical treatment. Monoclonal antibodies were anti-MAGE-A4 protein (57B), anti-HLA class I (EMR 8-5) and anti-CD8 (clone C8/144B). The reaction was evaluated as +++ (>50% stained cells), ++ (25–50%), + (5–25%), ± (1–5%) and − (<1%) for MAGE-A4 and HLA class I expression.

2.6. In vitro stimulation of CD4 and CD8 T cells

CD8 and CD4 T cells were purified from peripheral blood mononuclear cells (PBMCs) using CD8 Microbeads and a CD4+ T Cell Isolation Kit (Miltenyi Biotec). The remaining cells were used as antigen-presenting cells (APCs) after pulsing with a mixture of 31 MAGE-A4 overlapping peptides. Then, 5×10^5 CD4 or CD8 T cells were cultured with 10×10^5 APCs after irradiation with IL-2 (10 U/mL; Roche Diagnostics) and IL-7 (20 ng/mL; R&D Systems) for 21 days or 8 days, respectively. CD4 or CD8 T cells harvested were re-stimulated with T-APCs pulsed with a mixture of 31 MAGE-A4 overlapping peptides or HIV (p17, 39–51) peptide as the control for 6 h [32].

2.7. IFNγ intracellular staining (ICS)

ICS was performed with an ICS kit (BD Biosciences) according to the manufacturer's instructions followed by treatment with GolgiStop reagent containing monensin (BD Biosciences) for 1 h. Cells

Table 1
Immune responses and clinical responses following CHP-MAGE-A4 vaccination.

Patient ID	Immunization	MAGE-A4-specific immune response							
		Antibody[a]		CD4[b]		CD8[b]		Clinical response	OS (days)
		Pre	Post	Pre	Post	Pre	Post		
P-1	16	–	+	–	+	–	+	PD	218
P-2	13	–	–	–	–	–	–	PD	254
P-3	5	+	nd	nd		nd		NE	(74)
P-4	6	–	–	–	–	–	–	PD	82
P-5	7	+	+	–	–	–	+	PD	206
P-6	15	–	–	–	–	–	–	SD	228
P-7	31	–	++	–	+	–	+	PD	436
P-8	2	–	nd	nd		nd		NE	(42)
P-9	16	–	–	–	–	–	–	PD	340
P-10	7	–	–	–	–	–	–	PD	90
P-11	5	+	nd	nd		nd		NE	(81)
P-12	35	–	+	–	+	–	+	SD	767
P-13	7	–	–	–	–	–	–	PD	129
P-14	9	–	–	–	–	–	–	PD	179
P-15	7	–	–	–	–	–	+	PD	96
P-16	40	–	++	–	–	–	+	PD	1029
P-17	4	–	nd	nd		nd		NE	(63)
P-18	4	–	nd	nd		nd		NE	(66)
P-19	6	–	–	–	–	–	–	PD	92
P-20	7	+	+	–	–	–	–	PD	116

OS: overall survival; PD: progressive disease; SD: stable disease; NE: not evaluated; nd: not done.
[a] Antibody response was determined by ELISA. Antibody response shown here represents O.D. for MAGE-A4 protein: ++ ≥1.0; + >1.0 to ≥0.47; – >0.47.
[b] CD4 and CD8 T cell responses were determined by IFNγ intracellular cytokine staining with those cells stimulated in vitro once. IFNγ-positive cells: +++ >10%; ++ >5% to ≤10%; + >1% to ≤5%; – ≤1%.

were stained with CD8-V450 (clone RPA-T8; BD Biosciences), CD4-V450 (clone RPA-T4; BD Biosciences), CD3-Alexafluor 700 (clone UCHT1; BD Biosciences), eFluor 780-fixable viability dye (eBioscience, San Diego, CA) and IFNγ-FITC (clone 4S.B3; BD Biosciences).

2.8. Western blot

Recombinant protein (20 ng) in sample buffer was boiled for 5 min and subjected to SDS-PAGE with 10–20% polyacrylamide Bio-Rad Ready-Gels (Bio-Rad). After electrophoresis, the membrane was blocked with 5% FCS/PBS and then incubated with patients' sera diluted 1:100 for 1 h at room temperature. Horseradish peroxidase (HRP)-conjugated goat anti-human IgG (MBL) was added to the membrane. Signals were developed with a 5-bromo-4-chloro-3-indolylphosphate-nitroblue tetrazolium chromogenic substrate kit (Bio-Rad). Anti-MAGE-A4 monoclonal antibody (57B) used as the positive control at 1:200 dilution was given by Dr G.C. Spagnoli (University Hospital Basel, Basel, Switzerland).

2.9. Activated regulatory T cells in PBMC

Activated regulatory T cells (Treg) were analyzed by a flow cytometer using CD3-PerCPCy5.5 (clone OKT3; eBioscience), CD4-Alexafluor 700 (clone RPA-T4; eBioscience), CD8-V500 (clone RPA-T8; BD Biosciences), CD45RA-FITC (clone HI100; BD Biosciences), eFluor 780-fixable viability dye (eBioscience) and FoxP3-PE (clone 236A/E7; eBioscience). The details of the assay and the definition of activated Tregs were described previously [33].

2.10. Statistics analysis

Rates of the immune responses were compared by Fisher's exact test, and the survival curve was estimated using the Kaplan–Meier method and compared by the log-rank test. All analyses were performed using the SPSS statistical package, version 15.0 (SPSS Inc., Chicago, IL).

3. Results

3.1. Patient characteristics

Twenty advanced cancer patients were enrolled: 18 patients with esophageal cancer, a patient with lung cancer and a patient with gastric cancer expressing MAGE-A4 antigen (Supplementary Table). They received 2–40 immunizations and 15 patients completed a cycle of vaccination (Table 1).

3.2. Safety

Grade 1 fever and Grade 1 injection site reactions, e.g., skin redness or pruritus, were observed in 4 and 13 patients, respectively, after vaccination, and improved without any treatment (Supplementary Table). No severe adverse event was observed.

3.3. Clinical response

All patients underwent image analysis and routine physical checks during and after vaccination. An SD response was observed in two esophageal cancer patients, P-6 and P-12, out of 15 patients who completed vaccination (Table 1). In patient P-6, relapsed lymph node metastasis in the right neck after radical esophagectomy showed a 9% increase in its diameter after 6 immunizations with CHP-MAGE-A4. In patient P-12, although the main tumor disappeared after chemotherapy, metastasis in the left lung was observed with a 15% increase in its diameter after a cycle of vaccination. Both patients received additional cycles of CHP-MAGE-A4 vaccination; however, these target lesions showed rapid enlargement after the second cycle.

3.4. Monitoring of humoral immune response

MAGE-A4 antibody in sera obtained from all patients at baseline and 15 vaccine-completed patients two weeks after the final immunization were analyzed by ELISA. Four patients, P-3, P-5, P-11

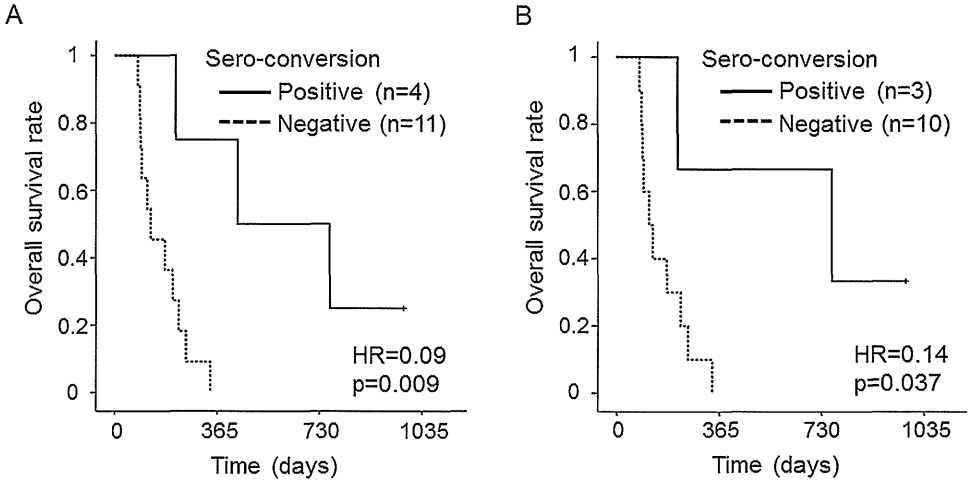

Fig. 1. Antibody production and prognosis. Overall survival of 15 patients and 13 esophageal cancer patients who completed 1 cycle of vaccination and the antibody response determined by ELISA were analyzed. Kaplan–Meier curves illustrate the duration of overall survival of sero-converted patients (solid line) and patients without an antibody response (dotted line) in 15 patients (A) and 13 esophageal cancer patients (B). The hazard ratio (HR) and log-rank *P* value for overall survival comparing patients with positive against negative antibody responses were calculated.

and P-20, showed the production of MAGE-A4 antibody at baseline (sero-positive) while others did not (sero-negative) (Table 1). After vaccination, 4 of 13 sero-negatives among 15 vaccine-completed patients showed increased O.D. values by ELISA and were considered positive serological responses (Supplementary Fig. 1A). No increased response was observed with sera from two sero-positives. These sero-conversions were observed just after a cycle of vaccination in all four patients. Anti-MAGE-A4, but not anti-His-tag, antibody responses in sera from patients P-1, P-12 and P-16 were analyzed by Western blot analysis using recombinant MAGE-A4 protein without any tags (Supplementary Fig. 1B).

Then, the overall survival after the first immunization in sero-conversion positives and negatives was analyzed in 15 vaccine-completed patients. The four sero-converted patients showed prolonged overall survival, significantly longer than that of patients without an antibody response after vaccination (Fig. 1A). When the analysis was limited to esophageal cancer patients, the overall survival of the three sero-converted patients was also significantly longer than that of patients without a MAGE-A4 antibody response (Fig. 1B).

3.5. Immunohistochemical analysis of MAGE-A4, MHC class I and CD8

Expression of MAGE-A4 and MHC Class I antigens on tumor cells was analyzed by IHC using formalin-fixed paraffin-embedded tumor tissues obtained from all enrolled patients (Supplementary Table). Among 15 vaccine-completed patients, high expression of MAGE-A4 (>25% tumor cells) and MHC class I (>5% tumor cells) was observed in tumor tissues from 12 and 12 patients, respectively. Then, we analyzed whether there is any relation between the expression of MAGE-A4 and MHC class I antigens on tumor cells and the induction of immune responses by CHP-MAGE-A4 vaccination. Four of eight patients with high expression of MAGE-A4 or MHC class I antigen on tumor cells showed an antibody response while no patients with low expression of either antigen on tumors showed an antibody response. High expression of both MAGE-A4 and MHC class I antigens was observed on tumor cells from sero-converted patients (Fig. 2A and B). Next, we analyzed whether there is any relation between the expression of those antigens and overall survival by CHP-MAGE-A4 vaccination. Patients with tumor cells expressing high MAGE-A4 or MHC class I antigen showed significantly longer overall survival than those with lower expressions (Fig. 2C and D).

3.6. Induction of MAGE-A4-specific CD4 and CD8 T cell responses

MAGE-A4-specific CD4 and CD8 T cell responses were analyzed by ICS assay using PBMCs obtained from 15 vaccine-completed patients at baseline and 2 weeks after the 6th immunization (Supplementary Fig. 2). MAGE-A4-specific IFNγ-producing CD4 and CD8 T cells were observed in no patient at baseline. After vaccination, induction of a CD4 T cell response was observed in three patients, P-1, P-7, P-12, who showed sero-conversion, and induction of a CD8 T cell response was observed in six patients, P-1, P-5, P-7, P-12, P-15, P-16, who showed antibody production (Table 1). Patients with induction of MAGE-A4-specific IFNγ-producing CD8 T cells, but not CD4 T cells, lived longer than those without induction (Supplementary Fig. 3).

3.7. Impact of CD4+ FoxP3 high+ regulatory T cells on overall survival

The ratio of CD4+ Foxp3 high+ cells in CD3+ T cells was analyzed using PBMCs obtained at baseline from 15 vaccine-completed patients. When the patients were divided by the mean of the ratio, the two SD patients, P-6 and P-12, belonged in the low ratio group (Supplementary Fig. 4A and B). Patients with a low ratio of CD4+ Foxp3 high+ cells in CD3+ T cells showed longer overall survival than patients with a high ratio after vaccination, although it was not significant (Supplementary Fig. 4C).

4. Discussion

We showed that the induction of MAGE-A4-specific immune responses correlated well with the prognosis of patients vaccinated with CHP-MAGE-A4. In our previous study of cancer vaccines with NY-ESO-1 protein [34–39], NY-ESO-1f peptide [40] and NY-ESO-1 overlapping peptide [41], feasible clinical responses were observed in several patients; however, we could not confirm the effects of NY-ESO-1 vaccines on the good prognosis of enrolled patients. There are several reports of successful cancer vaccines which prolonged the overall survival of vaccinated patients [42,43], and some studies revealed that patients with the induction of an antigen-specific CD8 T cell response, but not an antibody response,

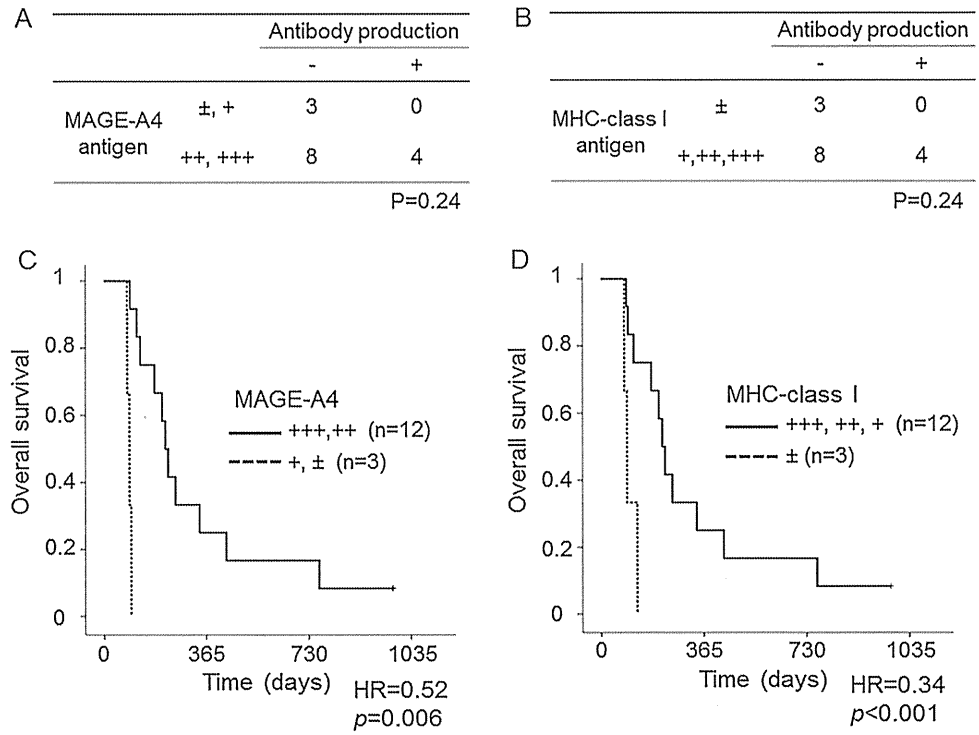

Fig. 2. MAGE-A4 and MHC-class antigen expression and prognosis. MAGE-A4 and MHC-class I were analyzed by immunohistochemical analysis with monoclonal antibodies; anti-pan-MAGE protein (57B), anti-human leukocyte antigen (HLA) class I (EMR 8–5). The reaction was evaluated as +++ (>50% stained cells), ++ (25–50%), + (5–25%), ± (1–5%) and – (<1%) for MAGE-A4 and HLA class I expression. Among 15 vaccine-completed patients, tumor tissues from the four MAGE-A4 sero-converted patients showed higher expression of both MAGE-A4- and MHC-class I-antigens of tumor cells (A and B). The patients with tumor cells expressing higher MAGE-A4 or MHC-class I antigen showed a significantly longer overall survival than those with lower expressions (C and D).

survived longer [44]. Our results of immune monitoring indicated that the induction of not only MAGE-A4 CD8 T cells but also MAGE-A4 antibody responses could be a marker for predicting the good prognosis of patients vaccinated with MAGE-A4 protein. Detection of an antibody response is considered to be a useful tool for monitoring cancer vaccines with protein because it is easy to analyze with sera using ELISA [35]. In our previous studies of NY-ESO-1 antigen, specific humoral and cellular responses were spontaneously induced in patients with NY-ESO-1-expressing tumors, and elicited much more frequently and earlier in patients vaccinated with NY-ESO-1 than MAGE-A4 [39–41]. CT antigens, among tumor antigens, are known to have better immunogenicity because of their unique expression pattern [1]. However, MAGE-A4 antigen might not possess such strong immunogenicity as other CT antigens, for example, NY-ESO-1. Although it is not easy to determine and explain the intent of the immunogenicity of antigenic molecules, one possibility for determining immunogenicity is the immune competition by other molecules. The existence of ubiquitous expressions of other MAGE family members might interfere with the immune response of MAGE-A4 as a tumor antigen [3]. Another possibility is the stability of MHC and antigenic peptide complexes. It is reported that MAGE-A4 epitope peptide combined with HLA-A2 is less stable than Tax10 or influenza matrix epitope peptides but is consistent with common sets of A2-complexes determined by thermal denaturation measurements [15]. Nevertheless, the induction of a MAGE-A4 antibody response was a good marker of the long survival of patients vaccinated with MAGE-A4 protein, indicating that the immunogenicity of MAGE-A4 might be adequate to induce immune responses which can be used for immune monitoring to predict the prognosis of vaccinated patients.

To investigate which factors induce a humoral immune response by MAGE-A4 vaccine, the expression of MAGE-A4 and MHC class I antigens in tumor tissues was analyzed by IHC, and it was shown that the four sero-converted patients had cancers with high expression of both MAGE-A4 and MHC class I. Moreover, overall survival was prolonged in patients with tumors with high expression of MAGE-A4 antigen, suggesting that these patients might have elicited MAGE-A4-specific immune responses to some extent by MAGE-A4 vaccination, resulting in a good prognosis. The weak band observed in sero-negative patient P-16 at baseline by Western blot analysis (Supplementary Fig. 1B) might indicate such an undetectable level of MAGE-A4 immune responses by ELISA, probably due to the property of recombinant MAGE-A4 protein or MAGE-A4 antigen itself.

Next, we tried to find direct immunological activity against tumor cells, resulting in some clinical benefit, e.g., OS, progression-free survival, or tumor shrinkage. In two SD patients, while one showed sero-conversion but not the other, seromics analysis showed the antigen spreading among CT antigens in both patients after vaccination (Supplementary Fig. 5). In addition, activated regulatory T cells were abundantly observed in PBMC from both SD patients, although they did not influence OS. In our previous study of patients vaccinated with NY-ESO-1, antigen spreading was also observed [37], and Tregs were not increased after vaccination [41]. Antigen spreading of CTL against tumor-specific antigens after cancer vaccine with MAGE-1, 3 was also reported, indicating its contribution to tumor regression [45]. P-16 underwent resection of lung metastasis before and after vaccination, and both specimens were available for IHC analysis (Supplementary Fig. 6). Although the expressions of MAGE-A4 and MHC class I were consistent, the number of tumor-infiltrating CD8+ T cells after vaccination was twice as many as at the baseline.

In summary, CHP-MAGE-A4 vaccine was safe and two SD patients were observed. High expression of MAGE-A4 and MHC class I antigens in tumor cells and the induction of MAGE-A4 humoral and cellular immune responses would be feasible prognostic markers for patients vaccinated with MAGE-A4 protein.

Conflict of interest statement

All authors have declared that there are no financial conflicts of interest in regard to this work, but Hiroshi Shiku is a stockholder of ImmunoFrontier, Inc. CHP-MAGE-A4 reagent used in this study was supplied by ImmunoFrontier, Inc.

Acknowledgments

We thank Ms. Kayoko Maekawa for preparation of the manuscript, Mr Masahide Hamaguchi for the support of statistical analysis and Mr Daisuke Sugiyama and Ms Yukari Funabiki for techinical support. The study was supported by a Grant-in-Aid for Scientific Research (B) and the Project for the Development of Innovative Research on Cancer Therapeutics of the Ministry of Education, Culture Sports Science and Technology of Japan.

Appendix A. Supplementary data

Supplementary data associated with this article can be found, in the online version, at http://dx.doi.org/10.1016/j.vaccine.2014.09.002.

References

[1] Simpson AJG, Caballero OL, Jungbluth A, Chen Y-T, Old LJ. Cancer/testis antigens, gametogenesis and cancer. Nat Rev Cancer 2005;5:615–25.
[2] Caballero OL, Chen Y-T. Cancer/testis (CT) antigens: potential targets for immunotherapy. Cancer Sci 2009;100:2014–21.
[3] Nishikawa H, Maeda Y, Ishida T, Gnjatic S, Sato E, Mori F, et al. Cancer/testis antigens are novel targets of immunotherapy for adult T-cell leukemia/lymphoma. Blood 2012;119:3097–104.
[4] Cesson V, Rivals J-P, Escher A, Piotet E, Thielemans K, Posevitz V, et al. MAGE-A3 and MAGE-A4 specific CD4(+) T cells in head and neck cancer patients: detection of naturally acquired responses and identification of new epitopes. Cancer Immunol Immunother 2011;60:23–35.
[5] Vansteenkiste J, Zielinski M, Linder A, Dahabreh J, Gonzalez EE, Malinowski W, et al. Adjuvant MAGE-A3 immunotherapy in resected non-small-cell lung cancer: phase II randomized study results. J Clin Oncol 2013;31:2396–403.
[6] Tyagi P, Mirakhur B. MAGRIT: the largest-ever phase III lung cancer trial aims to establish a novel tumor-specific approach to therapy. Clin Lung Cancer 2009;10:371–4.
[7] Gnjatic S, Wheeler C, Ebner M, Ritter E, Murray A, Altorki NK, et al. Seromic analysis of antibody responses in non-small cell lung cancer patients and healthy donors using conformational protein arrays. J Immunol Methods 2009;341:50–8.
[8] Groeper C, Gambazzi F, Zajac P, Bubendorf L, Adamina M, Rosenthal R, et al. Cancer/testis antigen expression and specific cytotoxic T lymphocyte responses in non small cell lung cancer. Int J Cancer 2007;120:337–43.
[9] Kocher T, Zheng M, Bolli M, Simon R, Forster T, Schultz-Thater E, et al. Prognostic relevance of MAGE-A4 tumor antigen expression in transitional cell carcinoma of the urinary bladder: a tissue microarray study. Int J Cancer 2002;100:702–5.
[10] Yakirevich E, Sabo E, Lavie O, Resnick MB. Expression of the MAGE-A4 and NY-ESO-1 cancer-testis antigens in serous ovarian neoplasms expression of the MAGE-A4 and NY-ESO-1 cancer-testis antigens in serous ovarian neoplasms. Clin Cancer Res 2003;9:6453–60.
[11] Yoshida N, Abe H, Ohkuri T, Wakita D, Sato M, Noguchi D, et al. Expression of the MAGE-A4 and NY-ESO-1 cancer-testis antigens and T cell infiltration in non-small cell lung carcinoma and their prognostic significance. Int J Oncol 2006;28:1089–98.
[12] Bergeron A, Picard V, LaRue H, Harel F, Hovington H, Lacombe L, et al. High frequency of MAGE-A4 and MAGE-A9 expression in high-risk bladder cancer. Int J Cancer 2009;125:1365–71.
[13] Shigematsu Y, Hanagiri T, Shiota H, Kuroda K, Baba T, Mizukami M, et al. Clinical significance of cancer/testis antigens expression in patients with non-small cell lung cancer. Lung Cancer 2010;68:105–10.
[14] Laban S, Atanackovic D, Luetkens T, Knecht R, Busch C-J, Freytag M, et al. Simultaneous cytoplasmic and nuclear protein expression of MAGE-A family and NY-ESO-1 cancer-testis antigens represents an independent marker for poor survival in head & neck cancer. Int J Cancer 2014;135:1–11.
[15] Hillig RC, Coulie PG, Stroobant V, Saenger W, Ziegler A, Hülsmeyer M. High-resolution structure of HLA-A*0201 in complex with a tumour-specific antigenic peptide encoded by the MAGE-A4 gene. J Mol Biol 2001;310:1167–76.
[16] Jia Z-C, Ni B, Huang Z-M, Tian Y, Tang J, Wang J-X, et al. Identification of two novel HLA-A*0201-restricted CTL epitopes derived from MAGE-A4. Clin Dev Immunol 2010;2010:567594.
[17] Miyahara Y, Naota H, Wang L, Hiasa A, Goto M, Watanabe M, et al. Determination of cellularly processed HLA-A2402-restricted novel CTL epitopes derived from two cancer germ line genes, MAGE-A4 and SAGE. Clin Cancer Res 2005;11:5581–9.
[18] Zhang Y, Stroobant V, Russo V, Boon T, van der Bruggen P. A MAGE-A4 peptide presented by HLA-B37 is recognized on human tumors by cytolytic T lymphocytes. Tissue Antigens 2002;60:365–71.
[19] Ohkuri T, Wakita D, Chamoto K, Togashi Y, Kitamura H, Nishimura T. Identification of novel helper epitopes of MAGE-A4 tumour antigen: useful tool for the propagation of Th1 cells. Br J Cancer 2009;100:1135–43.
[20] Watson NFS, Ramage JM, Madjd Z, Spendlove I, Ellis IO, Scholefield JH, et al. Immunosurveillance is active in colorectal cancer as downregulation but not complete loss of MHC class I expression correlates with a poor prognosis. Int J Cancer 2006;118:6–10.
[21] Ishigami S, Natsugoe S, Nakajo A, Arigami T, Kitazono M, Okumura H, et al. HLA-class I expression in gastric cancer. J Surg Oncol 2008;97:605–8.
[22] Simpson JAD, Al-Attar A, Watson NFS, Scholefield JH, Ilyas M, Durrant LG. Intratumoral T cell infiltration, MHC class I and STAT1 as biomarkers of good prognosis in colorectal cancer. Gut 2010;59:926–33.
[23] Hanagiri T, Shigematsu Y, Shinohara S, Takenaka M, Oka S, Chikaishi Y, et al. Clinical significance of expression of cancer/testis antigen and down-regulation of HLA class-I in patients with stage I non-small cell lung cancer. Anticancer Res 2013;33:2123–8.
[24] Bukur J, Jasinski S, Seliger B. The role of classical and non-classical HLA class I antigens in human tumors. Semin Cancer Biol 2012;22:350–8.
[25] Lampen MH, van Hall T. Strategies to counteract MHC-I defects in tumors. Curr Opin Immunol 2011;23:293–8.
[26] Cabrera T, Lara E, Romero JM, Maleno I, Real LM, Ruiz-Cabello F, et al. HLA class I expression in metastatic melanoma correlates with tumor development during autologous vaccination. Cancer Immunol Immunother 2007;56:709–17.
[27] Carretero R, Romero JM, Ruiz-Cabello F, Maleno I, Rodriguez F, Camacho FM, et al. Analysis of HLA class I expression in progressing and regressing metastatic melanoma lesions after immunotherapy. Immunogenetics 2008;60:439–47.
[28] Gu XG, Schmitt M, Hiasa A, Nagata Y, Ikeda H, Sasaki Y, et al. A novel hydrophobized polysaccharide/oncoprotein complex vaccine induces in vitro and in vivo cellular and humoral immune responses against HER2-expressing murine sarcomas. Cancer Res 1998;58:3385–90.
[29] Eisenhauer EA, Therasse P, Bogaerts J, Schwartz LH, Sargent D, Ford R, et al. New response evaluation criteria in solid tumours: revised RECIST guideline (version 1.1). Eur J Cancer 2009;45:228–47.
[30] Trotti A, Colevas AD, Setser A, Rusch V, Jaques D, Budach V, et al. CTCAE v3.0: development of a comprehensive grading system for the adverse effects of cancer treatment. Semin Radiat Oncol 2003;13:176–81.
[31] Tanaka H, Miyazaki N, Matoba K, Nogi T, Iwasaki K, Takagi J. Higher-order architecture of cell adhesion mediated by polymorphic synaptic adhesion molecules neurexin and neuroligin. Cell Rep 2012;2:101–10.
[32] Nishikawa H, Sato E, Briones G, Chen L-M, Matsuo M, Nagata Y, et al. In vivo antigen delivery by a *Salmonella typhimurium* type III secretion system for therapeutic cancer vaccines. J Clin Invest 2006;116:1946–54.
[33] Sugiyama D, Nishikawa H, Maeda Y, Nishioka M, Tanemura A, Katayama I, et al. Anti-CCR4 mAb selectively depletes effector-type FoxP3+CD4+ regulatory T cells, evoking antitumor immune responses in humans. Proc Natl Acad Sci U S A 2013;110:17945–50.
[34] Uenaka A, Wada H, Isobe M, Saika T, Tsuji K, Sato E, et al. T cell immunomonitoring and tumor responses in patients immunized with a complex of cholesterol-bearing hydrophobized pullulan (CHP) and NY-ESO-1 protein. Cancer Immun 2007;7:9.
[35] Kawabata R, Wada H, Isobe M, Saika T, Sato S, Uenaka A, et al. Antibody response against NY-ESO-1 in CHP-NY-ESO-1 vaccinated patients. Int J Cancer 2007;120:2178–84.
[36] Fujiwara S, Wada H, Kawada J, Kawabata R, Takahashi T, Fujita J, et al. NY-ESO-1 antibody as a novel tumour marker of gastric cancer. Br J Cancer 2013;108:1119–25.
[37] Kawada J, Wada H, Isobe M, Gnjatic S, Nishikawa H, Jungbluth AA, et al. Heteroclitic serological response in esophageal and prostate cancer patients after NY-ESO-1 protein vaccination. Int J Cancer 2012;130:584–92.
[38] Tsuji K, Hamada T, Uenaka A, Wada H, Sato E, Isobe M, et al. Induction of immune response against NY-ESO-1 by CHP-NY-ESO-1 vaccination and immune regulation in a melanoma patient. Cancer Immunol Immunother 2008;57:1429–37.
[39] Wada H, Sato E, Uenaka A, Isobe M, Kawabata R, Nakamura Y, et al. Analysis of peripheral and local anti-tumor immune response in esophageal cancer patients after NY-ESO-1 protein vaccination. Int J Cancer 2008;123:2362–9.
[40] Kakimi K, Isobe M, Uenaka A, Wada H, Sato E, Doki Y, et al. A phase I study of vaccination with NY-ESO-1f peptide mixed with Picibanil OK-432 and Montanide ISA-51 in patients with cancers expressing the NY-ESO-1 antigen. Int J Cancer 2011;129:2836–46.
[41] Wada H, Isobe M, Kakimi K, Mizote Y, Eikawa S, Sato E, et al. Vaccination with NY-ESO-1 overlapping peptides mixed with picibanil OK-432 and montanide

ISA-51 in patients with cancers expressing the NY-ESO-1 antigen. J Immunother 2014;37:84–92.
[42] Schwartzentruber DJ, Lawson DH, Richards JM, Conry RM, Miller DM, Treisman J, et al. Gp100 peptide vaccine and interleukin-2 in patients with advanced melanoma. N Engl J Med 2011;364:2119–27.
[43] Kono K, Iinuma H, Akutsu Y, Tanaka H, Hayashi N, Uchikado Y, et al. Multicenter, phase II clinical trial of cancer vaccination for advanced esophageal cancer with three peptides derived from novel cancer-testis antigens. J Transl Med 2012;10:141.
[44] Walter S, Weinschenk T, Stenzl A, Zdrojowy R, Pluzanska A, Szczylik C, et al. Multipeptide immune response to cancer vaccine IMA901 after single-dose cyclophosphamide associates with longer patient survival. Nat Med 2012;18:1254–61.
[45] Corbière V, Chapiro J, Stroobant V, Ma W, Lurquin C, Lethé B, et al. Antigen spreading contributes to MAGE vaccination-induced regression of melanoma metastases. Cancer Res 2011;71:1253–62.

Vaccine 32 (2014) 957–964

Contents lists available at ScienceDirect

Vaccine

journal homepage: www.elsevier.com/locate/vaccine

Production of NY-ESO-1 peptide/DRB1*08:03 tetramers and ex vivo detection of CD4 T-cell responses in vaccinated cancer patients

Yu Mizote[a,b], Akiko Uenaka[c], Midori Isobe[b], Hisashi Wada[d], Kazuhiro Kakimi[e], Takashi Saika[f], Shoichi Kita[g], Yukari Koide[g], Mikio Oka[b], Eiichi Nakayama[c,*]

[a] Department of Immunology, Okayama University Graduate School of Medicine, Dentistry and Pharmaceutical Sciences, Okayama, Japan
[b] Department of Respiratory Medicine, Kawasaki Medical School, Okayama, Japan
[c] Faculty of Health and Welfare, Kawasaki University of Medical Welfare, Kurashiki 701-0193, Okayama, Japan
[d] Department of Surgery, Osaka University Graduate School of Medicine, Osaka, Japan
[e] Department of Immunotherapeutics, University of Tokyo Hospital, Tokyo, Japan
[f] Department of Urology, Okayama University Graduate School of Medicine, Dentistry and Pharmaceutical Sciences, Okayama, Japan
[g] Medical & Biological Laboratories, Nagano, Japan

ARTICLE INFO

Article history:
Received 27 June 2013
Received in revised form 17 October 2013
Accepted 18 December 2013
Available online 5 January 2014

Keywords:
Tumor immunology
NY-ESO-1
CD4 T-cell
MHC class II tetramer

ABSTRACT

We established CD4 T-cell clones, Mz-1B7, and Ue-21, which recognized the NY-ESO-1 121–138 peptide from peripheral blood mononuclear cells (PBMCs) of an esophageal cancer patient, E-2, immunized with an NY-ESO-1 protein and determined the NY-ESO-1 minimal epitopes. Minimal peptides recognized by Mz-1B7 and Ue-21 were NY-ESO-1 125–134 and 124–134, respectively, both in restriction to DRB1*08:03. Using a longer peptide, 122–135, and five other related peptides, including either of the minimal epitopes recognized by the CD4 T-cell clones, we investigated the free peptide/DR recognition on autologous EBV-B cells as APC and peptide/DR tetramer binding. The results showed a discrepancy between them. The tetramers with several peptides recognized by either Mz-1B7 or the Ue-21 CD4 T-cell clone did not bind to the respective clone. On the other hand, unexpected binding of the tetramer with the peptide not recognized by CD4 T-cells was observed. The clone Mz-1B7 did not recognize the free peptide 122–135 on APC, but the peptide 122–135/DRB1*08:03 tetramer bound to the TCR on those cells. The failure of tetramer production and the unexpected tetramer binding could be due to a subtly modified structure of the peptide/DR tetramer from the structure of the free peptide/DR molecule. We also demonstrated that the NY-ESO-1 123–135/DRB1*08:03 tetramer detected ex vivo CD4 T-cell responses in PBMCs from patients after NY-ESO-1 vaccination in immunomonitoring.

1. Introduction

To analyze T-cell immunomonitoring after vaccination, peptide/MHC tetramers have become widely used [1]. Peptide/MHC tetramers identified and visualized antigen specific T-cells. MHC class I tetramers were originally developed by Altman and Davis [2], and used for various antigens including those of viral or tumor origin [3,4]. However, MHC class II tetramers have been used in only a few studies because of the difficulty in preparation [5]. The soluble form of MHC class II molecules is necessary to produce tetramers. However, production of such molecules using extracellular domains of MHC class II α and β chains is generally difficult because of a lack of assembly or aggregation [6]. These findings indicate the necessity of transmembrane regions for the proper assembly of the molecules. Kalandadze et al. [7] found that replacement of the hydrophobic transmembrane regions by the Fos and Jun leucine zipper dimerization motifs resulted in the assembly and secretion of DRαβ heterodimers in yeast. Novak et al. [8] developed MHC class II tetramers using DR molecules incorporating leucin zipper motifs to stabilize the DRα and β heterodimer. The procedure has been widely used, but successful production of MHC class II tetramers is still limited [9–13].

We recently analyzed CD4 T-cell responses against NY-ESO-1 in PBMCs from patients who were vaccinated with a complex of cholesterol-bearing hydrophobized pullulan and NY-ESO-1 protein (CHP-NY-ESO-1) in our clinical trial and determined three novel NY-ESO-1 CD4 T-cell epitopes: NY-ESO-1 87–100 bound to DRB1*09:01, NY-ESO-1 95–107 bound to DQB1*04:01, and NY-ESO-1 124–134 bound to DRB1*08:03 [14]. CD4 T-cells that

Abbreviations: APC, antigen-presenting cell; CHP-NY-ESO-1, complex of cholesterol-bearing hydrophobized pullulan and NY-ESO-1 whole protein; Fmoc, *N*-(9-fluorenyl)-methoxycarbonyl; HD, healthy donor; MFI, mean fluorescence intensity; OLP, overlapping peptide; PBMC, peripheral blood mononuclear cell.

* Corresponding author. Tel.: +81 86 462 1111x54954; fax: +81 86 464 1109.
E-mail address: nakayama@mw.kawasaki-m.ac.jp (E. Nakayama).

0264-410X/$ – see front matter © 2013 Elsevier Ltd. All rights reserved.
http://dx.doi.org/10.1016/j.vaccine.2013.12.042

recognized these epitope peptides also recognized EBV-B cells or DC that were treated with recombinant NY-ESO-1 protein or an NY-ESO-1-expressing tumor cell lysate, suggesting that the epitope peptides are naturally processed. These CD4 T-cells had a cytokine profile with Th1 characteristics.

In this study, we showed that tetramers with several peptides recognized by the CD4 T-cell clones did not bind to the same clones. On the other hand, unexpected binding of the tetramer with a peptide not recognized by CD4 T-cells was observed. The failure of tetramer production and the unexpected tetramer binding could be due to a subtly modified structure of the peptide/DR tetramer from the structure of the free peptide/DR molecule. We also demonstrated that the NY-ESO-1 123–135/DRB1*08:03 tetramer detected ex vivo CD4 T-cell responses in PBMCs from patients after NY-ESO-1 vaccination in immunomonitoring.

2. Materials and methods

2.1. Patients and blood samples

Peripheral blood samples were drawn from esophageal cancer patients E-1 and E-2, and a prostate cancer patient P-3, who were vaccinated with CHP-NY-ESO-1, and a lung cancer patient TK-OLP-01, who was vaccinated with NY-ESO-1 OLP in our clinical trials [15,16] after obtaining written informed consent. PBMCs were isolated by density gradient centrifugation using Histopaque 1077 (Sigma–Aldrich, St. Louis, MO). CD4 T-cells and $CD19^+$ cells were purified from PBMCs using CD4 and CD19 microbeads, respectively, using a large scale column and a magnetic device (Miltenyi Biotec, Auburn, CA). The cells were stored in liquid N_2 until use. HLA typing was done using PBMCs with a sequence-specific oligo-nucleotide probe and sequence-specific priming of genomic DNA using standard procedures. Patient E-2 was found to possess homozygous alleles.

2.2. Peptides

Peptides were synthesized using standard solid-phase methods based on *N*-(9-fluorenyl)-methoxycarbonyl (Fmoc) chemistry on a Multiple Peptide Synthesizer (AMS422, ABIMED, Langenfeld, Germany) at Okayama University (Okayama, Japan).

2.3. Cell lines

E-2 bulk CD4 T-cells were stimulated in vitro twice as described previously [14]. Clones were then established by limiting dilution. EBV-B cells were generated from $CD19^+$ peripheral blood B cells using the culture supernatant from EBV-producing B95-8 cells.

2.4. Generation of HLA-DRB1*08:03 tetramers

HLA-DR tetramers were prepared as described previously [5]. The cDNA coding for the extracellular domains of the HLA-DRα chain was inserted by fusion PCR in a basic leucine zipper and His tag. The HLA-DRβ chain was fused with an acidic leucine zipper and the BirA substrate peptide for BirA enzyme-dependent biotinylation. The HLA-DRα and HLA-DRβ chimeric cDNA were cloned into the pcDNA3.1 vector, respectively. The expression vectors containing the HLA-DRα and HLA-DRβ chains were co-transfected into CHO cells.

2.5. ELISA

Supernatants (100 μl) from cultures of CD4 T-cells (5×10^3) stimulated for 18 h with autologous EBV-B cells (5×10^3) pre-pulsed for 30 min with peptide in a 96-well round bottomed culture plate, or with solid-phase peptide/HLA-DRB1*08:03 tetramers in a 96-well flat bottomed culture plate, were collected and the amounts of IFNγ were estimated by sandwich ELISA [14]. TNFα, IL-4, IL-10 and IL-17A in the culture supernatants were estimated by DuoSet Sandwich ELISAs (R&D Systems, Minneapolis, MN), according to the manufacturer's instructions.

2.6. Flow cytometry

FITC-conjugated anti-human TCRαβ mAb (BD), PerCP Cy5.5-conjugated anti-human CD3 mAb and APC-conjugated anti-human CD4 mAb (eBioscience, San Diego, CA) were used for T-cell surface staining. The stained cells were detected by FACS Canto II (BD). Flow cytometry results were analyzed with FlowJo (Tree Star, Ashland, OR).

2.7. Tetramer staining

CD4 T-cells were incubated with tetramers for 1 h at 37 °C in a 5% CO_2 atmosphere. FITC-conjugated anti-human CD4 mAb (Miltenyi Biotec) was added at the end of tetramer staining and incubated for an additional 20 min at 4 °C.

2.8. IFNγ capture assay

The method has been described previously [14].

2.9. TCR Vβ and CDR3 sequence analysis

For TCR Vβ analysis, the IOTest Beta Mark kit (Beckman Coulter, Brea, CA) was used. The CDR3 sequence was determined by PCR as described previously [17].

3. Results

3.1. Determination of NY-ESO-1 minimal epitopes recognized by CD4 T-cell clones Mz-1B7 and Ue-21 established from PBMCs of an esophageal cancer patient E-2 immunized with CHP-NY-ESO-1

We established CD4 T-cell clones from PBMCs of an esophageal cancer patient E-2 immunized with CHP-NY-ESO-1 which recognized the 18-mer NY-ESO-1 121–138 peptide. The CD4 T-cell clones Mz-1B7 and Ue-21 produced IFNγ, TNFα, but not IL-4, IL-10 or IL-17A (Supplementary Fig. 1), indicating that they have Th1 characteristics. We determined restriction molecules by antibody blocking and minimal epitopes using various N- and C-termini truncated peptides. Assays were done by ELISA examining IFNγ in the culture supernatant from responding T-cells using autologous EBV-B cells as antigen-presenting cells (APC). As shown in Fig. 1A, recognition of the 18-mer NY-ESO-1 121–138 by CD4 T-cell clones Mz-1B7 and Ue-21 was inhibited by addition of anti-HLA-DR mAb, but not anti-HLA-DQ mAb. Since patient E-2 possessed homozygous haplotypes (DRB1*08:03, DQA1*01:03, DQB1*06:01, DPB1*05:01) according to genetic analysis (see Section 2), the two clones Mz-1B7 and Ue-21 recognized the NY-ESO-1 peptide 121–138 in restriction to DRB1*08:03.

We then investigated recognition of various N- and C-termini truncated peptides and found that a core peptide region recognized by either clone Mz-1B7 or clone Ue-21 was made up of amino acids 125–134 (Fig. 1B). Further analysis revealed that a minimal peptide recognized by clone Mz-1B7 was peptide 125–134 (10-mer) and that recognized by clone Ue-21 was peptide 124–134 (11-mer) (Fig. 1C). Thus, clones Mz-1B7 and Ue-21 recognized

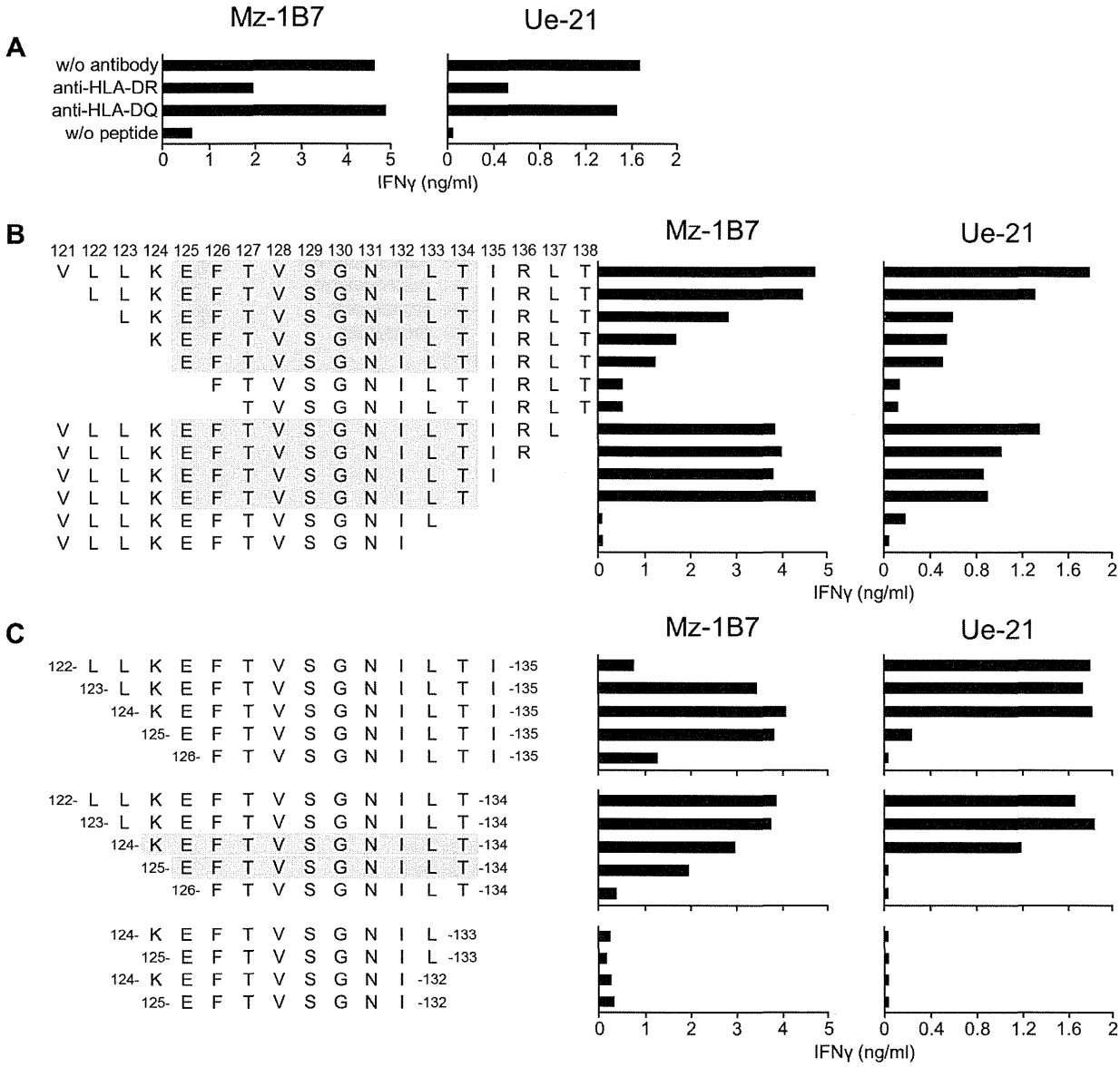

Fig. 1. Antibody blocking (A) and determination of NY-ESO-1 minimal epitopes ((B) and (C)) recognized by E-2 CD4 T-cell clones Mz-1B7 and Ue-21. In (A), CD4 T-cell clones (5×10^3) were stimulated for 18 h with autologous EBV-B cells (5×10^3) in the presence of NY-ESO-1 121–138 (VLLKEFTVSGNILTIRLT) peptide (100 nM), and anti-HLA-DR or anti-HLA-DQ mAb (5 μg/ml) in the culture. IFNγ in the culture supernatants was determined by ELISA. In B and C, CD4 T-cell clones (5×10^3) were stimulated for 18 h with autologous EBV-B cells (5×10^3) in the presence of truncated NY-ESO-1 121–138 peptides (100 nM). The core peptide region and each minimal epitopes recognized by CD4 T-cell clones are shown in gray boxes. IFNγ in the culture supernatants was determined by ELISA.

closely related, but different, minimal NY-ESO-1 peptides in restriction to the same DRB1*08:03. Recognition of closely related, but different, peptides by these CD4 T-cell clones was further confirmed with responses to other peptides. Peptide 122–135 was recognized by Ue-21, but not Mz-1B7. On the other hand, peptide 125–135 and peptide 126–135 were recognized by Mz-1B7, but not Ue-21.

3.2. Differential recognition by clone Mz-1B7 and clone Ue-21 of the longer peptide 122–135, including minimal epitopes recognized by either clone

To confirm that the longer peptide 122–135 was recognized by only clone Ue-21, but not clone Mz-1B7, irrespective of including epitopes recognized by either clone, an IFNγ capture assay together with ELISA was performed examining IFNγ in the same culture stimulated with peptide 122–135 and five other related peptides using autologous EBV-B cells as APC as above. As shown in Fig. 2A, a response of clone Mz-1B7 was observed against the peptides 123–135, 124–135, 122–134, 123–134 and 124–134, but not 122–135 in either the IFNγ capture assay or ELISA. No response against peptide 122–135 was observed up to a peptide concentration of 100 nM in ELISA. On the other hand, a response of clone Ue-21 was observed against all of the peptides used. These results were consistent with the results shown in Fig. 1.

3.3. Tetramer binding

We produced tetramers using the longer peptide 122–135, and five other related peptides 123–135, 124–135, 122–134, 123–134 and 124–134. The DR molecule was constructed by combining the DRA*01:01 and DRB1*08:03 chains that fused the leucine zipper motif at the C-terminal ends [8]. In the DRA locus, seven alleles DRA*01:01:01:01, DRA*01:01:01:02,

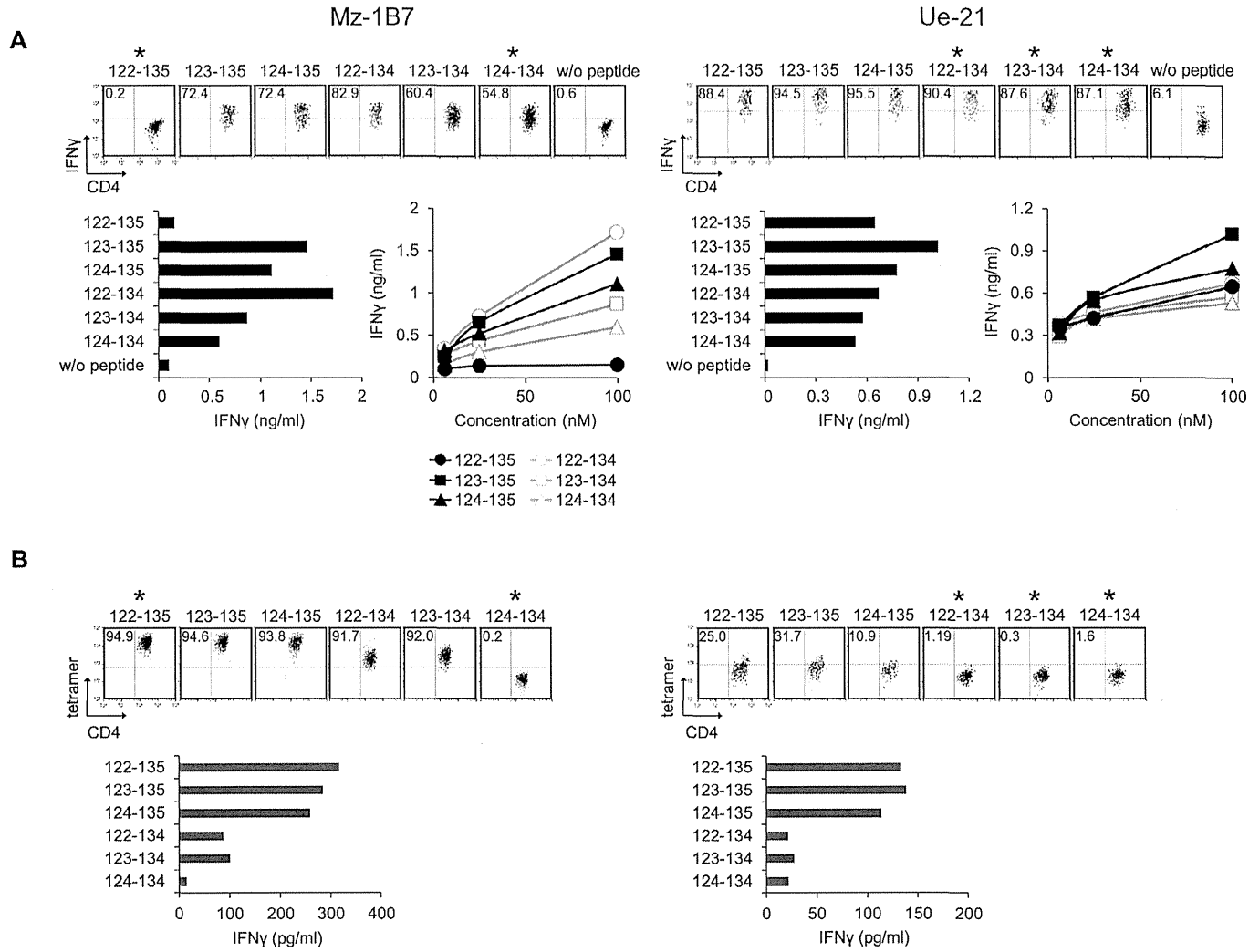

Fig. 2. Discrepancy between peptide recognition (A) and tetramer binding (B) in E-2 CD4 T-cell clones Mz-1B7 and Ue-21. In A top, CD4 T-cell clones (1×10^4) were stimulated for 4 h with the indicated peptides (1 μM) using autologous EBV-B cells (1×10^4) as APC. IFNγ-secreting CD4 T-cells were determined by an IFNγ capture assay using FACS Canto II. In A bottom, CD4 T-cell clones (5×10^3) were stimulated for 18 h with autologous EBV-B cells (5×10^3) pre-pulsed for 30 min with the indicated peptides (100 nM) (left) or with graded concentrations (6.25, 25 or 100 nM) of the indicated peptides (right). IFNγ in the culture supernatant was determined by ELISA. In B top, CD4 T-cell clones were stained with the indicated peptide/HLA-DRB1*08:03 tetramers (5 μg/ml) at 37 °C for 1 h followed by staining with an anti-CD4 mAb, and analyzed using FACS Canto II. In B bottom, CD4 T-cell clones (5×10^3) were stimulated for 18 h with the indicated peptide/HLA-DRB1*08:03 tetramers coated on wells in microculture plates. IFNγ in the culture supernatant was determined by ELISA. The peptides that show a discrepancy between recognition (A) and tetramer binding (B) are marked by *.

DRA*01:01:01:03, DRA*01:01:02, DRA*01:02:01, DRA*01:02:02 and DRA*01:02:03 have been identified. These alleles differ only at amino acid 217 in the cytoplasmic domain, which is included in the region replaced by a leucin zipper motif from amino acid residue 152 in the α2 domain. Therefore, any DRA allele can be used for tetramer production.

With these six peptide/DR tetramers, we examined binding to clones Mz-1B7 and Ue-21. As shown in Fig. 2B, to clone Mz-1B7, binding of tetramers with peptide 122–135, 123–135, 124–135, 122–134 and 123–134, but not 124–134, was observed. The peptide 122–135 including the minimal epitope 125–134 was not recognized by Mz-1B7, but a tetramer constructed using the same peptide bound to Mz-1B7. Furthermore, peptide 124–134 that also included the minimal epitope 125–134 was recognized by Mz-1B7, but a tetramer constructed using the same peptide did not bind to the same clone.

On the other hand, to clone Ue-21, weak binding of tetramers with peptides 122–135, 123–135 and 124–135, but only marginal binding of tetramers with 122–134, 123–134 or 124–134, was observed. The peptides 122–134 and 123–134, including the minimal epitope 124–134 and the peptide124–134 itself, were recognized by Ue-21, but the tetramers constructed using the same peptides bound to the same clone only marginally. IFNγ production by CD4 T-cell clones in stimulation with the tetramers was consistent with tetramer binding (Fig. 2B bottom).

We further examined the only marginal binding of a tetramer constructed using the peptide 124–134 to Mz-1B7 and Ue-21 under different culture conditions. As shown in Fig. 3A and B, efficient binding of the tetramer constructed using the peptide 123–135 to clone Mz-1B7 was observed at 25–37 °C after incubation for 10–120 min. However, only marginal binding was observed with the tetramer constructed using the peptide 124–134, even at 37 °C after incubation for 120 min. Only marginal binding of the tetramer with the peptide 124–134 to Mz-1B7 or Ue-21 was observed up to a concentration of 10 μg/ml (Fig. 3C and D).

3.4. Expression of CD4 and TCR on CD4 T-cell clones

Expression of CD4, CD3 and TCRαβ was analyzed by FACS. As shown in Fig. 4A, expression of CD4 was observed similarly on clones Mz-1B7 and Ue-21. On the other hand, expression of CD3 and TCRαβ was observed on Ue-21 strongly, but on Mz-1B7

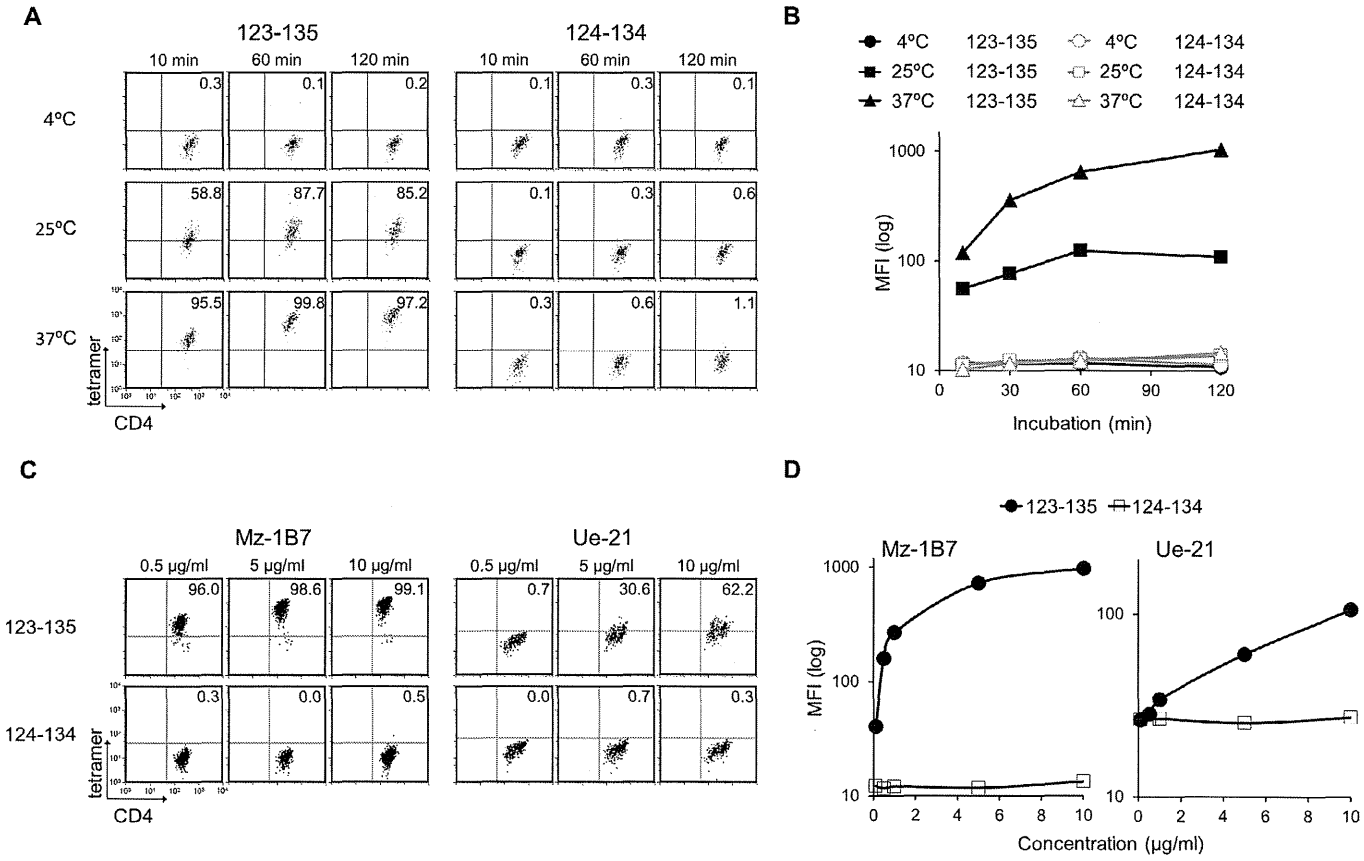

Fig. 3. Effect of temperature, incubation time and dose in tetramer staining. In (A) and (B), the E-2 CD4 T-cell clone Mz-1B7 was stained with NY-ESO-1 123–135 (LKEFTVSGNILTI) or NY-ESO-1 124–134 (KEFTVSGNILT) peptide/HLA-DRB1*08:03 tetramers (5 μg/ml) at 4, 25 or 37 °C for 10, 30, 60 or 120 min followed by staining with anti-CD4 mAb. In C and D, E-2 CD4 T-cell clones Mz-1B7 and Ue-21 were stained with NY-ESO-1 123–135 (LKEFTVSGNILTI) or NY-ESO-1 124–134 (KEFTVSGNILT) peptide/HLA-DRB1*08:03 tetramers (0.5, 1, 5 or 10 μg/ml) at 37 °C for 1 h followed by staining with an anti-CD4 mAb. Analysis was done using FACS Canto II. Dot plots (A and C) and the mean fluorescence intensity (MFI) (B and D) of tetramer staining are shown.

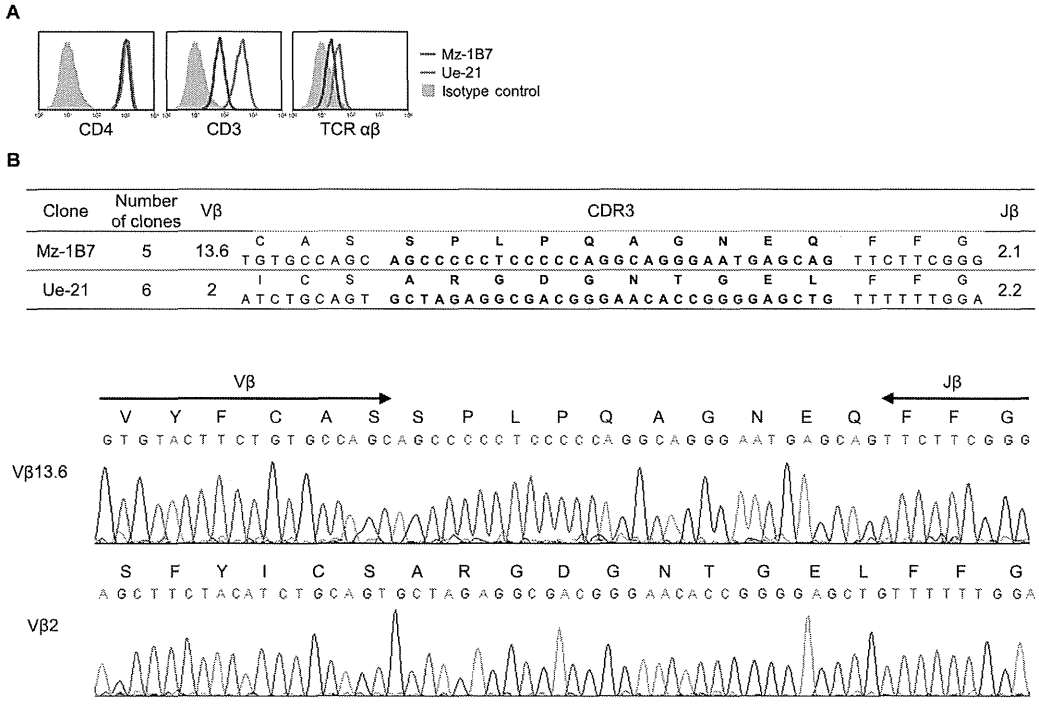

Fig. 4. Surface expression of the molecules on CD4 T-cell clones (A) and analysis of CDR3 sequences (B). In A, CD4 T-cell clones Mz-1B7 and Ue-21 stained with anti-CD4, CD3 and TCRαβ mAb were analyzed using FACS Canto II. In B, the nucleotide sequence and deduced amino acid sequences of the V–D–J junctional region of TCR β chain from the E-2 CD4 T-cell clones are shown.

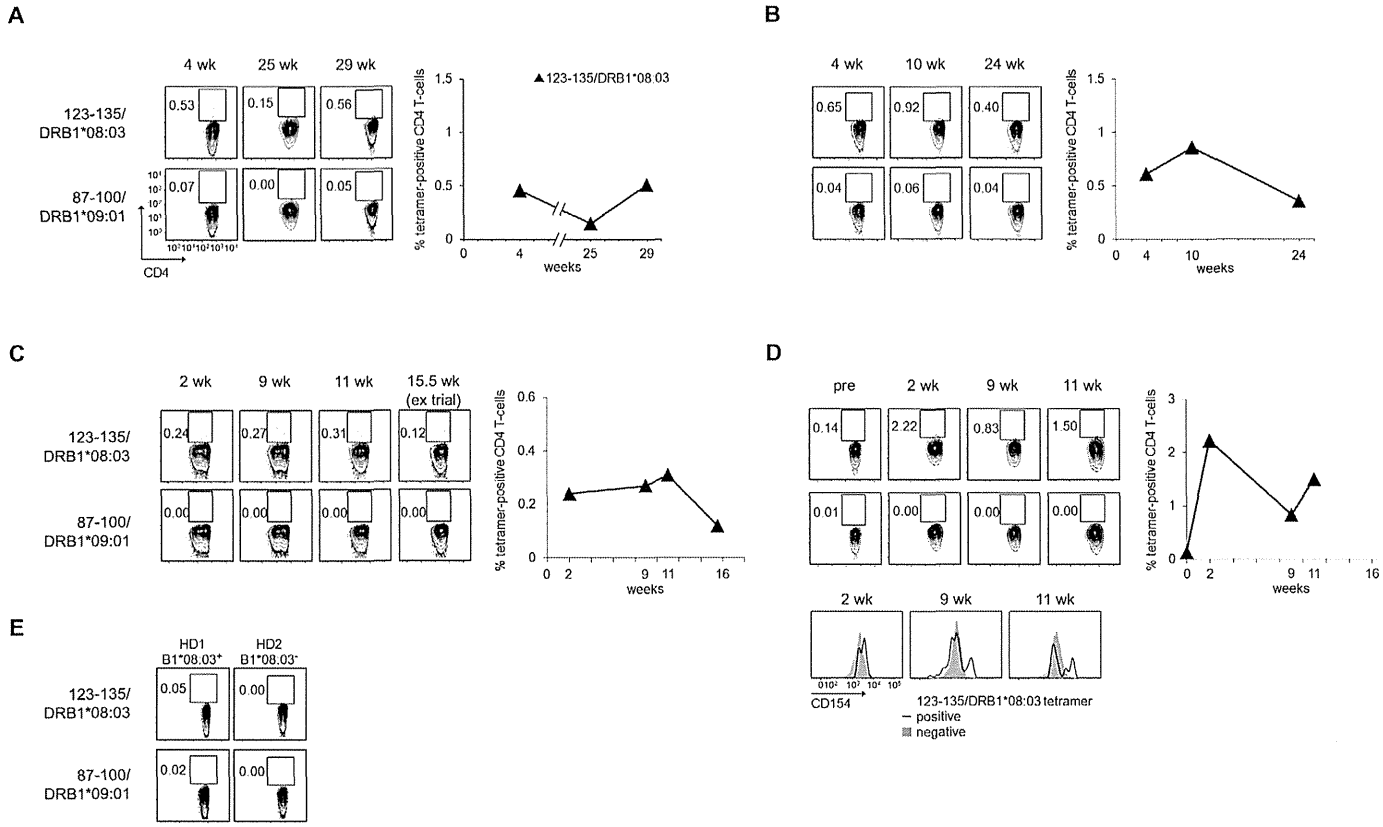

Fig. 5. Immunomonitoring of CD4 T-cell responses by the tetramer in cancer patients immunized with NY-ESO-1. CD4 T-cells from prostate cancer patient P-3 (A) and esophageal cancer patient E-1 (B) who were immunized with CHP-NY-ESO-1, and a lung cancer patient TK-OLP-01 (C) who was immunized with NY-ESO-1 OLP were stained ex vivo with the NY-ESO-1 123–135/HLA-DRB1*08:03 tetramer or a control NY-ESO-1 87–100/HLA-DRB1*09:01 tetramer (5 μg/ml) at 37 °C for 1 h followed by staining with an anti-CD4 mAb. In D, TK-OLP01 CD4 T-cells after in vitro stimulation twice were stained with the NY-ESO-1 123–135/HLA-DRB1*08:03 tetramer or a control NY-ESO-1 87–100/HLA-DRB1*09:01 tetramer and anti-CD154 mAb at 37 °C for 2 h followed by staining with an anti-CD4 mAb. The histogram shows CD154 expression on NY-ESO-1 123–135/DRB1*08:03 tetramer-positive (open) and negative (filled) CD4 T-cells. CD4 T-cells from two HDs were stained with tetramers as a negative control (E). HD1 and HD2 are DRB1*08:03-positive and -negative individuals, respectively. Analysis was done using FACS Canto II.

moderately. As shown in Fig. 4B, analysis of CDR3 sequences revealed that clone Mz-1B7 utilizes the Vβ13.6, SPLPQAGNEQ sequence for CDR3 and Jβ2.1. On the other hand, clone Ue-21 utilizes the Vβ2, ARGDGNTGEL sequence for CDR3 and Jβ2.2.

By cloning bulk CD4 T-cells from the E-2 patient, we obtained 58 DRB1*08:03-restricted clones. Within these, 5 clones utilized Vβ13.6 and 53 clones Vβ2. 5 clones with Vβ13.6 and 6 clones with Vβ2 were sequenced for CDR3. A combination of the same CDR3 sequence and Jβ was utilized by clones with each Vβ, respectively.

3.5. Monitoring of CD4 T-cell response by a tetramer constructed using the peptide 123–135 in cancer patients immunized with NY-ESO-1

Tetramers constructed using the peptide 123–135 (NY-ESO-1 123–135/DRB1*08:03) were used to monitor CD4 T-cell responses in DRB1*08:03-expressing cancer patients immunized with CHP-NY-ESO-1, or a mixture of NY-ESO-1 OLPs (NY-ESO-1 79–108, 100–129, 121–150 and 142–173) with Picibanil and Montanide. As shown in Fig. 5, the tetramer detected positive cells ex vivo in CD4 T-cells from PBMCs of a prostate cancer patient (P-3) (Fig. 5A) and an esophageal cancer patient (E-1) (Fig. 5B) who expressed DRB1*08:03 after immunization with CHP-NY-ESO-1. The tetramer also detected positive cells in CD4 T-cells from PBMCs of a lung cancer patient (TK-OLP-01) immunized with NY-ESO-1 OLP ex vivo (Fig. 5C) and after in vitro stimulation (Fig. 5D). Predominant detection of tetramer NY-ESO-1 123–135/DRB1*08:03-positive cells was observed after in vitro stimulation. Induction of CD154 (CD40L) expression on tetramer-positive cells was examined. At 9 and 11 weeks (3 and 4 vaccinations) after immunization, CD154 (CD40L)-positive cells were detected in tetramer NY-ESO-1 123–135/DRB1*08:03-positive, but not negative, cells suggesting their activation. No tetramer-positive cells were detected in CD4 T-cells from DRB1*08:03-positive or negative healthy donors (HD) (Fig. 5E). No clonal analysis of CD4 T-cells was possible because PBMCs from these patients were not available for further study.

4. Discussion

In this study, we demonstrated that HLA class II tetramers produced using minimal epitope peptides efficiently recognized by CD4 T-cell clones did not bind to cognate CD4 T-cell clones. Furthermore, we showed that a tetramer produced using a peptide which included the epitope sequence, but was not recognized by the cognate CD4 T-cell clone, could bind to the same CD4 T-cell clone.

It has long been observed that production of HLA class II tetramers is extremely difficult when compared to the production of MHC class I tetramers [5,6]. HLA class II tetramers produced using minimal epitope peptides and HLA class II molecules dimerized by a leucine zipper motif incorporated in the molecule generally failed to bind cognate CD4 T-cell clones. There have been only a few reports of successful binding of MHC class II tetramers to CD4 T-cells in which long peptides which were recognized by those T-cells were used for tetramer production [9–11].

The reason for the difficulty in producing MHC class II tetramers has generally been considered to be due to inappropriate accommodation of the peptide in the groove of the MHC class II molecule, resulting in unnatural conformation. One of the constraints for MHC class II tetramer production is derived from the ambiguity of determining epitopes for CD4 T-cells. Peptides with the addition of various lengths of N- and C-terminal ends to the minimal core sequence are recognized by CD4 T-cells. Moreover, it is difficult to determine whether the minimal peptide is a naturally presenting epitope or not [18,19]. Lack of accurate information about natural HLA class II epitopes appears to be one of the reasons for the difficulty in HLA class II tetramer production.

Moreover, low binding affinity/avidity of the peptide to MHC class II molecules may also be involved. In this study, we confirmed successful tetramer production with differential retention time by HPLC. For example, the prolongation of the retention time was 0.554 min with the addition of the 12-mer NY-ESO-1 123–134 peptide (LKEFTVSGNILT) to the DRB1*08:03 monomer, but was 0.039 min with the addition of a negative control peptide to DRB1*08:03. The prolongation of the retention time was 0.246 min with the positive control 15-mer CLIP peptide (PVSKMRMATPLLMQA). However, the possibilities discussed above were also considered for the failure to produce a tetramer using the minimal epitope peptides. First, the use of an inappropriate epitope may have been involved. Defining the precise length of natural epitopes bound to class II molecules is extremely difficult as described above. Second, the epitope peptide may have weak binding affinity for the MHC class II molecules used for tetramer production (see below). With the core 9-mer peptides bound to HLA-DRB1*08:03, hydrophobic residues at P1 as phenylalanine (F) or tyrosine (Y) and residues at P6 as proline (P), serine (S), arginine (R) or asparagine (N) are relevant as anchor residues [20,21]. F at position 126 and N at position 131 in NY-ESO-1 121–138 may contribute to binding. Addition of isoleucine (I) at position 135 strongly stabilized tetramer production. Third, binding instability of the peptide to class II molecules may also be involved.

In addition to the failure to produce MHC class II tetramers using the epitope peptides, this study showed unexpected binding of the tetramer with a peptide not recognized by CD4 T-cells. The clone Mz-1B7 did not recognize the free peptide 122–135 on autologous EBV-B cells as APC, but the peptide 122–135/DRB1*08:03 tetramer bound to the TCR on those cells. The possibility of a lack of binding of the free peptide 122–135 to the DRB1*08:03 molecule on autologous APC is unlikely because clone Ue-21 recognized it efficiently. Rather, the tetramer binding could be due to a subtly modified structure of the 122–135 peptide/DRB1*08:03 tetramer from the structure of the free 122–135 peptide/DRB1*08:03 molecule. This could result from structural modification of either the peptide or the DR molecule, or both, during preparation of the peptide/DR tetramer, or simply be due to a subtle conformational change in the DR molecule itself due to fusion of the leucine zipper motif [8]. In the latter, it is possible that association of DRα and DRβ chains by the leucine zipper motif on each chain caused a subtle difference in the conformation of the natural DR molecule, although there was no convincing evidence to support this idea in this study.

Here, we also demonstrated that the NY-ESO-1 123–135/DRB1*08:03 tetramer detected ex vivo CD4 T-cell responses in PBMCs from a prostate cancer patient P-3 and an esophageal cancer patient E-1 after CHP-NY-ESO-1 vaccination, and a lung cancer patient TK-OLP-01 after NY-ESO-1 OLP vaccination. These patients possessed the DRB1*08:03 allele. Patient P-3 was positive for the NY-ESO-1 antibody before vaccination (sero-positive) and patients E-1 and TK-OLP-01 were sero-negative [15]. In these patients, tetramer-positive CD4 T-cells were detected after vaccination.

Based on the discussion above, a possible difference in CD4 T-cell clones recognizing the epitope peptides from those detected by the respective peptide/HLA class II tetramer should be taken into consideration in HLA class II tetramer analysis.

Acknowledgments

We thank Ms. Junko Mizuuchi for preparation of the manuscript. This work was supported, in part, by a Grant-in-Aid for Scientific Research (B) from the Ministry of Education, Culture, Sports, Science and Technology of Japan, and by New Energy and Industrial Technology Development Organization (NEDO), Japan.

Conflict of interest: There is no conflict of interest.

Appendix A. Supplementary data

Supplementary material related to this article can be found, in the online version, at http://dx.doi.org/10.1016/j.vaccine.2013.12.042.

References

[1] Guillaume P, Dojcinovic D, Luescher IF. Soluble MHC-peptide complexes: tools for the monitoring of T cell responses in clinical trials and basic research. Cancer Immunity 2009;9.
[2] Altman JD, Moss PA, Goulder PJ, Barouch DH, McHeyzer-Williams MG, Bell JI, et al. Phenotypic analysis of antigen-specific T lymphocytes. Science 1996;274:94–6.
[3] Bakker AH, Schumacher TNM. MHC multimer technology: current status and future prospects. Current Opinion in Immunology 2005;17:428–33.
[4] Chattopadhyay PK, Melenhorst JJ, Ladell K, Gostick E, Scheinberg P, Barrett AJ, et al. Techniques to improve the direct ex vivo detection of low frequency antigen-specific CD8+ T cells with peptide-major histocompatibility complex class I tetramers. Cytometry Part A 2008;73:1001–9.
[5] Cecconi V, Moro M, Del Mare S, Dellabona P, Casorati G. Use of MHC class II tetramers to investigate CD4+ T cell responses: problems and solutions. Cytometry Part A 2008;73:1010–8.
[6] Vollers SS, Stern LJ. Class II major histocompatibility complex tetramer staining: progress, problems, and prospects. Immunology 2008;123:305–13.
[7] Kalandadze A, Galleno M, Foncerrada L, Strominger JL, Wucherpfennig KW. Expression of recombinant HLA-DR2 molecules. Journal of Biological Chemistry 1996;271:20156.
[8] Novak EJ, Liu AW, Nepom GT, Kwok WW. MHC class II tetramers identify peptide-specific human CD4+ T cells proliferating in response to influenza A antigen. Journal of Clinical Investigation 1999;104:R63.
[9] James EA, LaFond R, Durinovic-Bello I, Kwok W. Visualizing antigen specific CD4+ T cells using MHC class II tetramers. Journal of Visualized Experiments 2009.
[10] Nepom GT, Buckner JH, Novak EJ, Reichstetter S, Reijonen H, Gebe J, et al. HLA class II tetramers: tools for direct analysis of antigen-specific CD4+ T cells. Arthritis & Rheumatism 2002;46:5–12.
[11] Wooldridge L, Lissina A, Cole DK, Van Den Berg HA, Price DA, Sewell AK. Tricks with tetramers: how to get the most from multimeric peptide-MHC. Immunology 2009;126:147–64.
[12] Ayyoub M, Dojcinovic D, Pignon P, Raimbaud I, Schmidt J, Luescher I, et al. Monitoring of NY-ESO-1 specific CD4+ T cells using molecularly defined MHC class II/His-tag-peptide tetramers. Proceedings of the National Academy of Sciences 2010;107:7437.
[13] Ayyoub M, Pignon P, Dojcinovic D, Raimbaud I, Old LJ, Luescher I, et al. Assessment of vaccine-induced CD4 T cell responses to the 119–143 immunodominant region of the tumor-specific antigen NY-ESO-1 using DRB1* 0101 tetramers. Clinical Cancer Research 2010;16:4607.
[14] Mizote Y, Taniguchi T, Tanaka K, Isobe M, Wada H, Saika T, et al. Three novel NY-ESO-1 epitopes bound to DRB1* 0803, DQB1* 0401 and DRB1* 0901 recognized by CD4 T cells from CHP-NY-ESO-1-vaccinated patients. Vaccine 2010;28:5338–46.
[15] Uenaka A, Wada H, Isobe M, Saika T, Tsuji K, Sato E, et al. T cell immunomonitoring and tumor responses in patients immunized with a complex of cholesterol-bearing hydrophobized pullulan (CHP) and NY-ESO-1 protein. Cancer Immunity 2007;7.
[16] Wada H, Sato E, Uenaka A, Isobe M, Kawabata R, Nakamura Y, et al. Analysis of peripheral and local anti-tumor immune response in esophageal cancer patients after NY-ESO-1 protein vaccination. International Journal of Cancer 2008;123:2362–9.
[17] Genevée C, Diu A, Nierat J, Caignard A, Dietrich PY, Ferradini L, et al. An experimentally validated panel of subfamily-specific oligonucleotide primers (V_α1-w29/V_β1-w24) for the study of human T cell receptor variable V gene segment usage by polymerase chain reaction. European Journal of Immunology 1992;22:1261–9.

[18] Chicz RM, Urban RG, Gorga JC, Vignali DA, Lane WS, Strominger JL. Specificity and promiscuity among naturally processed peptides bound to HLA-DR alleles. Journal Experimental Medicine 1993;178:27–47.
[19] Chicz RM, Urban RG, Lane WS, Gorga JC, Stern LJ, Vignali DA, et al. Predominant naturally processed peptides bound to HLA-DR1 are derived from MHC-related molecules and are heterogeneous in size. Nature 1992;358:764–8, a–z index.
[20] Rapin N, Hoof I, Lund O, Nielsen M. The MHC motif viewer: a visualization tool for MHC binding motifs. Current Protocols in Immunology 2010. Chapter 18:Unit 18.17.
[21] Southwood S, Sidney J, Kondo A, del Guercio M-F, Appella E, Hoffman S, et al. Several common HLA-DR types share largely overlapping peptide binding repertoires. The Journal of Immunology 1998;160:3363–73.

Ann Surg Oncol (2014) 21:2105–2112
DOI 10.1245/s10434-014-3503-2

Annals of
SURGICAL ONCOLOGY
OFFICIAL JOURNAL OF THE SOCIETY OF SURGICAL ONCOLOGY

ORIGINAL ARTICLE – UROLOGIC ONCOLOGY

Prognostic Significance of CD204-Positive Macrophages in Upper Urinary Tract Cancer

Takashi Ichimura, MD[1], Teppei Morikawa, MD, PhD[1], Taketo Kawai, MD, PhD[2], Tohru Nakagawa, MD, PhD[2], Hirokazu Matsushita, MD, PhD[3], Kazuhiro Kakimi, MD, PhD[3], Haruki Kume, MD, PhD[2], Shumpei Ishikawa, MD, PhD[4], Yukio Homma, MD, PhD[2], and Masashi Fukayama, MD, PhD[1]

[1]Department of Pathology, Graduate School of Medicine, The University of Tokyo, Tokyo, Japan; [2]Department of Urology, Graduate School of Medicine, The University of Tokyo, Tokyo, Japan; [3]Department of Immunotherapeutics (Medinet), The University of Tokyo Hospital, Tokyo, Japan; [4]Department of Genomic Pathology, Medical Research Institute, Tokyo Medical and Dental University, Tokyo, Japan

ABSTRACT

Background. Evidence suggests that CD204-positive ($CD204^+$) tumor-infiltrating macrophages are associated with aggressive behavior of various cancers; however, the clinical, pathological, and prognostic associations of tumor-infiltrating $CD204^+$ macrophages in urothelial cancer have not been reported.

Methods. A tissue microarray was constructed from the centers and peripheries of 171 upper urinary tract cancers treated with nephroureterectomy. CD204 immunohistochemistry was performed. The density of $CD204^+$ cells was calculated using image analysis software, and survival analyses were performed using the Kaplan–Meier method and multivariate Cox proportional hazards regression models.

Results. High $CD204^+$ cell density at the centers and peripheries of tumors was significantly associated with several adverse prognostic factors, including sessile architecture, histological high-grade, presence of lymphovascular invasion, concomitant carcinoma in situ, higher tumor stage, and lymph node metastasis. High $CD204^+$ cell density was significantly associated with shorter metastasis-free and cancer-specific survival (log-rank $p < 0.001$) and shorter metastasis-free survival in multivariate analysis.

Conclusions. A high density of tumor-infiltrating $CD204^+$ macrophages was associated with aggressive behavior of upper urinary tract cancer. Our results suggest that a specific immune microenvironment may be associated with the biological behavior of urothelial cancer and that CD204 may serve as a novel prognostic biomarker for these tumors.

Tumor tissue comprises variable numbers of cancer and stromal cells, and the tumor microenvironment plays important roles in the biological behavior of cancer.[1–6] Macrophages, which contribute to the host's immune response, are the most abundant stromal cells in tumors.[7] Macrophages possess tumor suppressive (M1) and tumor-supportive (M2) functions.[8] M2-polarized macrophages express high levels of CD204 (also called scavenger receptor A).[9] Recent studies show that a high number of tumor-infiltrating CD204-positive ($CD204^+$) macrophages is associated with worse patient outcome in a variety of cancers.[10–16] However, the role of $CD204^+$ macrophages in urothelial cancer has not been reported. We therefore examined the clinicopathological and prognostic associations of tumor-infiltrating $CD204^+$ macrophages in patients with upper urinary tract cancer.

MATERIALS AND METHODS

Study Population

A total of 171 patients with upper urinary tract cancer who underwent nephroureterectomy at The University of Tokyo Hospital from 1996 to 2012 were included in this study. No

Electronic supplementary material The online version of this article (doi:10.1245/s10434-014-3503-2) contains supplementary material, which is available to authorized users.

First Received: 24 July 2013;
Published Online: 4 February 2014

M. Fukayama, MD, PhD
e-mail: mfukayama-tky@umin.org

patient received neoadjuvant chemotherapy. In 31 cases, bladder cancer was found and treated before or at the time of nephroureterectomy. All research protocols in the present study were approved by our Institutional Review Board.

Histopathological Evaluation

Hematoxylin and eosin (H&E)-stained slides of all cases were reviewed by a pathologist (TM) without knowledge of clinical outcomes. Tumor histology and grade were defined according to the World Health Organization/International Society of Urologic Pathology consensus classification.[17] All tumors (103 pelvic cancers and 68 ureteral cancers) were histologically diagnosed as urothelial carcinomas. Tumors were staged according to the TNM classification system.[18] Lymphovascular invasion was examined using H&E and Elastica van Gieson staining.

Tissue Microarray Construction

H&E-stained slides were evaluated for the presence of the tumor center and the periphery. The tumor periphery was defined as the area of invasive margin or as the area where cancer cells were closest to the lamina propria for non-invasive tumors. For each tumor specimen, H&E-stained slides containing the tumor center and the periphery were selected. Using a tissue microarrayer (Beecher Instruments Inc., Sun Prairie, WI, USA), each region in the donor paraffin block was cored with a needle 2 mm in diameter and transferred to the recipient paraffin block.[19]

Immunohistochemical Analysis

Preparation of sections from paraffin blocks was performed as previously described.[20] Immunohistochemical analysis of CD204 was performed using a mouse monoclonal antibody against human CD204 (clone SRA-E5, 1:500; Transgenic, Kumamoto, Japan) according to standard techniques for a Ventana Benchmark® XT Autostainer (Ventana Medical Systems, Tucson, AZ, USA). Antigen retrieval was carried out using Cell Conditioning Solution (CC1-Tris-based EDTA buffer, pH 8.0; Ventana Medical Systems). Visualization was achieved using the I-VIEW DAB Universal Kit (Ventana Medical Systems) and hematoxylin counterstaining.

Image Analysis

Images of immunostained slides were digitized at 20× magnification using the NanoZoomer Digital Pathology (NDP) System (Hamamatsu Photonics, Hamamatsu, Japan). For digital quantification, image analysis software (Tissue Studio v.3.5; Definiens AG, Munich, Germany) was used to distinguish the $CD204^+$ macrophages.[21] The percentage of the area containing $CD204^+$ cells (summed area with $CD204^+$ cells/total measured area × 100) was calculated for each tissue microarray core.[14]

Statistical Analysis

All statistical analyses were performed using SAS software (Version 9.3, SAS Institute, Cary, NC, USA). All p values were two-sided. Differences were considered significant at $p < 0.05$. For categorical data, the Chi square test was performed. The Kaplan–Meier method and log-rank test were used to analyze survival. To control for confounding variables, multivariate Cox proportional hazards regression models were used. The multivariate models initially included gender, age at diagnosis, tumor side, tumor location, tumor architecture, tumor grade, lymphovascular invasion, concomitant carcinoma in situ, tumor stage, lymph node metastasis, and adjuvant chemotherapy. Tumor stage was dichotomized (pTa–pT1 vs. pT2–pT4) to be consistent with previous studies.[22–26] A backward elimination was performed using a threshold of $p = 0.05$; however, CD204 status, tumor stage, and lymph node metastasis were forced into the final models.

RESULTS

Distribution of Tumor-Infiltrating $CD204^+$ Macrophages in Upper Urinary Tract Cancer

Representative photomicrographs of CD204 immunohistochemistry are presented in Fig. 1. The median tumor-infiltrating $CD204^+$ cell density was 0.64 % (range 0.03–9.29 %) at the tumor center, and 0.81 % (range 0.03–12.43 %) at the tumor periphery. $CD204^+$ cell density of the two areas correlated positively (Spearman $r = 0.76$; $p < 0.0001$), and there was no significant difference between the tumor center and the periphery ($p > 0.05$, Wilcoxon signed-rank test). We divided the cases into high and low $CD204^+$ groups according to the median value of $CD204^+$ cell density.[14] High $CD204^+$ density at both the tumor center and the periphery was significantly associated with sessile architecture, histological high-grade, presence of lymphovascular invasion, concomitant carcinoma in situ, higher tumor stage, and lymph node metastasis (Table 1).

$CD204^+$ Macrophages and Clinical Outcome of Upper Urinary Tract Cancer

Patients with previous or concurrent bladder cancer ($n = 31$) were excluded from the survival analyses because

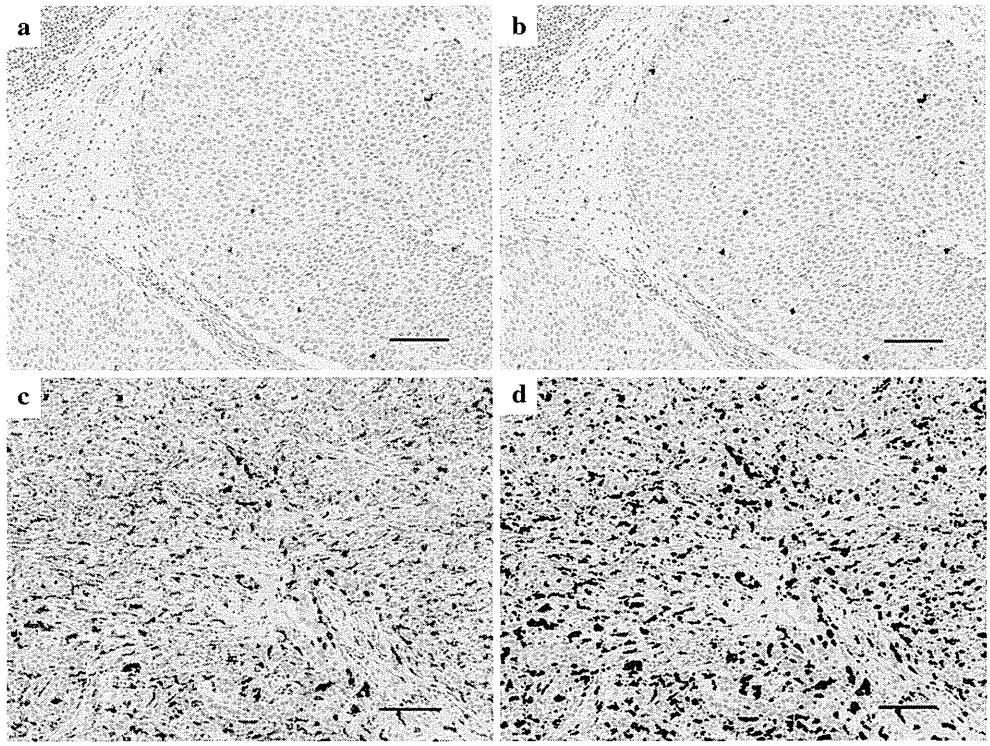

FIG. 1 Quantitation of $CD204^+$ macrophage density in upper urinary tract urothelial carcinoma. CD204 immunohistochemistry shows low (**a**) and high (**c**) infiltration of $CD204^+$ macrophages. Using image analysis software, immunopositive areas are highlighted in red, and the percentage of immunopositive area (summed area with $CD204^+$ macrophages/total measured area × 100) was calculated (**b**, **d**). *Bars* indicate 100 μm. *$CD204^+$* CD204-positive

they may affect the outcome of upper urinary tract cancer.[27] Among the 140 patients without bladder cancer at the time of nephroureterectomy, there were 58 bladder recurrences, 32 metastases, and 23 cancer-specific deaths during a median 56-month follow-up (interquartile range 25–86 months).

Kaplan–Meier analysis revealed that high $CD204^+$ density at both the tumor center and the periphery was significantly associated with shorter metastasis-free and cancer-specific survival (log-rank $p < 0.001$; Fig. 2). High $CD204^+$ density at both the tumor center and the periphery was also significantly associated with shorter metastasis-free survival in univariate and multivariate Cox models (Table 2). High $CD204^+$ density was significantly associated with shorter cancer-specific survival in univariate analysis, but the statistical significance was not achieved in multivariate analysis (Table 3). Lymphovascular invasion and lymph node metastasis were also significantly associated with shorter metastasis-free and cancer-specific survival in univariate and multivariate analyses. Tumor stage was not significantly associated with shorter metastasis-free and cancer-specific survival in multivariate analysis, consistent with previous studies.[24–26,28] $CD204^+$ density was not significantly associated with bladder recurrence-free survival in Kaplan–Meier analysis (Fig. 2) or in univariate and multivariate Cox models (Supplementary Table 1).

DISCUSSION

To our knowledge, the present study is the first to assess the clinicopathological and prognostic associations of $CD204^+$ macrophages in upper urinary tract cancer. We found that a high density of tumor-infiltrating $CD204^+$ cells was significantly associated with sessile architecture, histological high-grade, lymphovascular invasion, concomitant carcinoma in situ, higher tumor stage, and lymph node metastasis, which are adverse prognostic factors in upper urinary tract cancer.[29,30] Moreover, high $CD204^+$ cell density was significantly associated with shorter metastasis-free and cancer-specific survival. Our findings suggest that tumor-infiltrating $CD204^+$ macrophages are associated with aggressive behavior of upper urinary tract cancer.

A high density of tumor-infiltrating $CD204^+$ macrophages is associated with a poorer prognosis in lung,[10,12,13] pancreatic,[11,14,15] and esophageal carcinomas.[16] In two of these studies, the independent prognostic significance of CD204 expression was also shown using multivariate analysis.[12,14] In contrast, there was no prognostic